

SUMIS: Near-Optimal Soft-In Soft-Out MIMO Detection With Low and Fixed Complexity

Mirsad Čirkić and Erik G. Larsson
Communication Systems Division
Department of Electrical Engineering (ISY)
Linköping University, SE-581 83 Linköping, Sweden
{mirsad.cirkic,erik.g.larsson}@liu.se

Abstract—The fundamental problem of our interest here is soft-input soft-output multiple-input multiple-output (MIMO) detection. We propose a method, referred to as subspace marginalization with interference suppression (SUMIS), that yields unprecedented performance at low and fixed (deterministic) complexity. Our method provides a well-defined tradeoff between computational complexity and performance. Apart from an initial sorting step consisting of selecting channel-matrix columns, the algorithm involves no searching nor algorithmic branching; hence the algorithm has a completely predictable run-time and allows for a highly parallel implementation. We numerically assess the performance of SUMIS in different practical settings: full/partial channel state information, sequential/iterative decoding, and low/high rate outer codes. We also comment on how the SUMIS method performs in systems with a large number of transmit antennas.

I. INTRODUCTION

We consider multiple-input multiple-output (MIMO) systems, which are known to have high spectral efficiency in rich scattering environments [1] and high link robustness. A major difficulty in the implementation of MIMO systems is the detection (signal separation) problem, which is generally computationally expensive to solve. This problem can be especially pronounced in large MIMO systems, see [2]–[7] and the references therein. The complexity of the optimal detector, which computes the log-likelihood ratio (LLR) values exactly and therefore solves the MIMO detection problem optimally, grows exponentially with the number of transmit antennas and polynomially with the size of the signal constellation. The main difficulty in MIMO detection is the occurrence of ill-conditioned channels. Suboptimal and fast methods, such as zero-forcing, perform well only for well-conditioned channels. With coded transmission, if the channel is ill-conditioned and there is no coding across multiple channel realizations, using the zero-forcing detector can result in large packet error probabilities. Dealing with ill-conditioned channels is difficult and requires sophisticated techniques.

This work was supported in part by the Swedish Research Council (VR), the Swedish Foundation of Strategic Research (SSF), and the Excellence Center at Linköping-Lund in Information Technology (ELLIIT). Parts of this work were presented at the IEEE International Conference on Acoustics, Speech, and Signal Processing (ICASSP) 2012. The authors believe in reproducible research and will upload the C++ code as supplementary material (media) on IEEEXplore.

Many different methods have been proposed during the past two decades that aim to achieve, with reduced computational complexity, the performance of the optimal detector [8]–[19]. A concise exposition of some state-of-the-art MIMO detection technique can be found in [8] and a more extensive overview is given in [9]. Detection methods based on lattice reduction are explained in some detail in [10]. Most of today’s state-of-the-art detectors provide the possibility of trading complexity for performance via the choice of some user parameter. One important advantage of such detectors is that this parameter can be adaptively chosen depending on the channel conditions, in order to improve the overall performance [20], [21].

There are two main categories of MIMO detectors. The first consists of detectors whose complexity (run-time) depends on the particular channel realization. This category includes, in particular, methods that perform a tree-search. Notable examples include the sphere-decoding (SD) aided max-log method and its many relatives [14]–[18]. A recent method in this category is the reduced dimension maximum-likelihood search (RD-MLS) [9], [14]. Unfortunately, these methods have an exponential worst-case complexity unless a suboptimal termination criterion is used. The other category of detectors consists of methods that have a fixed (deterministic) complexity that does not depend on the channel realization. These methods are more desirable from an implementation point of view, as they eliminate the need for data buffers and over-dimensioning (for the worst-case) of the hardware. Examples of such detectors are the reduced dimension maximum a posteriori (RDMAP) method [11], the partial marginalization (PM) method [12], and the fixed-complexity SD (FCSD) aided max-log method [13]. These fixed-complexity detectors provide a simple and well-defined tradeoff between computational complexity and performance, they have a fixed and fully predictable run-time, and they are highly parallelizable. We will discuss existing detectors in more detail in Section II-B.

Summary of Contributions: We propose a new method that is inspired by the ideas in [11]–[14] of partitioning the original problem into smaller subproblems. As in the PM and RDMAP methods, we perform marginalization over a few of the bits when computing the LLR values. The approximate LLRs that enter the marginalization are much simpler than those in PM, and this substantially reduces the complexity of our algorithm, as will be explained in more

arXiv:1207.3316v3 [cs.IT] 31 Jan 2014

detail in Sec. III. In addition, we suppress the interference on the considered subproblems (subspaces) by performing soft interference suppression (SIS). The core idea behind SIS germinated in [22] in a different context than MIMO detection, but the use of SIS as a constituent of our proposed algorithm is mainly inspired by the work in [22]–[25]. The main differences between the SIS procedure used in our algorithm and that in [23]–[25] are: (i) we allow for the signal and interference subspaces to have varying dimensionality; (ii) we perform the SIS in a MIMO setting internally without the need for a priori information from the decoder, as opposed to [11], [23]; and (iii) we do not iterate the internal LLR values more than once, nor do we ignore the correlation between the interfering terms over the different receive antennas as in [24], [25]. We refer to our method as *subspace marginalization with interference suppression* (SUMIS). During the review of this paper, reference [26] was brought to our attention. Reference [26], published a year after SUMIS was first presented [27], discusses another variation on the theme where the interference is suppressed successively in contrast to SUMIS which does this in parallel.

SUMIS was developed with the primary objective not to require iteration with the channel decoder as this increases latency and complexity. However, SUMIS takes soft input, so the overall decoding performance can be improved by iterating with the decoder. The ideas behind SUMIS are fundamentally simple and allow for massively parallel algorithmic implementations. As demonstrated in Section VII, the computational complexity of SUMIS is extremely low, and the accuracy is near or better than that of max-log. SUMIS works well for both under- and over-determined MIMO systems.

This paper extends our conference paper [27] by including: a detailed complexity analysis, techniques for exploiting soft input (non-uniform a priori probabilities), and techniques for dealing with higher-order constellations and imperfect channel state information. In addition, we discuss and exemplify the applicability of SUMIS to systems with a large number of antennas.

II. PRELIMINARIES

We consider the real-valued MIMO-channel model

$$\mathbf{y} = \mathbf{H}\mathbf{s} + \mathbf{e}, \quad (1)$$

where $\mathbf{H} \in \mathbb{R}^{N_R \times N_T}$ is the MIMO channel matrix and $\mathbf{s} \in \mathcal{S}^{N_T}$ is the transmitted vector. We assume that $\mathcal{S} = \{-1, +1\}$ is a binary phase-shift keying (BPSK) constellation, hence referring to a “symbol” is equivalent to referring to a “bit”. With some extra expense of notation, as will be clear later, it is straightforward to extend all results that we present to higher order constellations. Furthermore, $\mathbf{e} \in \mathbb{R}^{N_R} \sim \mathcal{N}(\mathbf{0}, \frac{N_0}{2}\mathbf{I})$ denotes the noise vector and $\mathbf{y} \in \mathbb{R}^{N_R}$ is the received vector. The channel is perfectly known to the receiver unless stated otherwise. Also, hereinafter we assume that $N_R \geq N_T$ since this is typical in practice and simplifies the mathematics in the paper. Note that unlike many competing methods, SUMIS does not require $N_R \geq N_T$ —but this assumption is made to render the comparisons fair.

Throughout we think of (1) as an *effective channel model* for the MIMO transmission. In particular, if pure spatial multiplexing is used, the matrix \mathbf{H} in (1) just comprises the channel gains between all pairs of transmit and receive antennas. If linear precoding is used at the transmitter, then \mathbf{H} represents the combined effect of the precoding and the propagation channel. In the latter case, “transmit antennas” should be interpreted as “simultaneously transmitted streams”.

Note that with separable complex symbol constellations (quadrature amplitude modulation), every complex-valued model

$$\mathbf{y}_c = \mathbf{H}_c \mathbf{s}_c + \mathbf{e}_c, \quad \mathbf{e}_c \sim \mathcal{CN}(0, N_0 \mathbf{I}), \quad (2)$$

where $(\cdot)_c$ denotes the complex-valued counterparts of (1), can be posed as a real-valued model on the form (1) by setting

$$\mathbf{y} = \begin{bmatrix} \text{Re}\{\mathbf{y}_c\} \\ \text{Im}\{\mathbf{y}_c\} \end{bmatrix}, \quad \mathbf{s} = \begin{bmatrix} \text{Re}\{\mathbf{s}_c\} \\ \text{Im}\{\mathbf{s}_c\} \end{bmatrix}, \quad \mathbf{e} = \begin{bmatrix} \text{Re}\{\mathbf{e}_c\} \\ \text{Im}\{\mathbf{e}_c\} \end{bmatrix}, \quad (3a)$$

and

$$\mathbf{H} = \begin{bmatrix} \text{Re}\{\mathbf{H}_c\} & -\text{Im}\{\mathbf{H}_c\} \\ \text{Im}\{\mathbf{H}_c\} & \text{Re}\{\mathbf{H}_c\} \end{bmatrix}. \quad (3b)$$

We use the real-valued model throughout as we will later be partitioning \mathbf{H} into submatrices, and then the real-valued model offers some more flexibility: selecting one column in the representation (2) means simultaneously selecting two columns in the representation (1) (via (3)), which is more restrictive. Simulation results, not presented here due to lack of space, confirmed this with a performance advantage in working with the real-valued model. However, the difference is not major in most relevant cases. Disregarding this technicality, it is straightforward to re-derive all results in the paper using a complex-valued model instead. That could be useful, for example if M -ary phase-shift keying or some other non-separable signal constellation is used per antenna.

A. Optimal Soft MIMO Detection

The optimal soft information desired by the channel decoder is the a posteriori log-likelihood ratio $l(s_i|\mathbf{y}) \triangleq \log\left(\frac{P(s_i=+1|\mathbf{y})}{P(s_i=-1|\mathbf{y})}\right)$ where s_i is the i th bit of the transmitted vector \mathbf{s} . The quantity $l(s_i|\mathbf{y})$ tells us how likely it is that the i th bit of \mathbf{s} is equal to minus or plus one, respectively. By marginalizing out all bits except the i th bit in $P(\mathbf{s}|\mathbf{y})$ and using Bayes’ rule, the LLR becomes

$$\begin{aligned} l(s_i|\mathbf{y}) &= \log\left(\frac{\sum_{\mathbf{s}:s_i(\mathbf{s})=+1} P(\mathbf{s}|\mathbf{y})}{\sum_{\mathbf{s}:s_i(\mathbf{s})=-1} P(\mathbf{s}|\mathbf{y})}\right) \\ &= \log\left(\frac{\sum_{\mathbf{s}:s_i(\mathbf{s})=+1} p(\mathbf{y}|\mathbf{s})P(\mathbf{s})}{\sum_{\mathbf{s}:s_i(\mathbf{s})=-1} p(\mathbf{y}|\mathbf{s})P(\mathbf{s})}\right), \end{aligned} \quad (4)$$

where the notation $\sum_{\mathbf{s}:s_i(\mathbf{s})=x}$ means the sum over all possible vectors $\mathbf{s} \in \mathcal{S}^{N_T}$ for which the i th bit is equal to x . With uniform a priori probabilities, i.e., $P(\mathbf{s}) = 1/2^{N_T}$, the LLR

can be written as

$$\begin{aligned} l(s_i|\mathbf{y}) &= \log \left(\frac{\sum_{\mathbf{s}:s_i(\mathbf{s})=+1} p(\mathbf{y}|\mathbf{s})}{\sum_{\mathbf{s}:s_i(\mathbf{s})=-1} p(\mathbf{y}|\mathbf{s})} \right) \\ &= \log \left(\frac{\sum_{\mathbf{s}:s_i(\mathbf{s})=+1} \exp\left(-\frac{1}{N_0} \|\mathbf{y} - \mathbf{H}\mathbf{s}\|^2\right)}{\sum_{\mathbf{s}:s_i(\mathbf{s})=-1} \exp\left(-\frac{1}{N_0} \|\mathbf{y} - \mathbf{H}\mathbf{s}\|^2\right)} \right). \end{aligned} \quad (5)$$

In (4) and (5), there are 2^{N_T} terms that need to be evaluated and added. The complexity of this task is exponential in N_T and this is what makes MIMO detection difficult. Thus, many approximate methods have been proposed. One very good approximation of (5) is the so called max-log approximation [28],

$$l(s_i|\mathbf{y}) \approx \log \left(\frac{\max_{\mathbf{s}:s_i(\mathbf{s})=+1} \exp\left(-\frac{1}{N_0} \|\mathbf{y} - \mathbf{H}\mathbf{s}\|^2\right)}{\max_{\mathbf{s}:s_i(\mathbf{s})=-1} \exp\left(-\frac{1}{N_0} \|\mathbf{y} - \mathbf{H}\mathbf{s}\|^2\right)} \right), \quad (6)$$

where only the largest terms in each sum of (5) are retained, i.e., the terms for which $\|\mathbf{y} - \mathbf{H}\mathbf{s}\|$ is as small as possible. Typically, for numerical stability, sums as in (5) are evaluated by repeated use of the Jacobian logarithm: $\log(e^a + e^b) = \max(a, b) + \log(1 + e^{-|a-b|})$, where the second term can be tabulated as function of $|a - b|$. Max-log can then be viewed as a special case where the second term in the Jacobian logarithm is neglected. Note that even though max-log avoids the summation, one needs to search over 2^{N_T} terms to find the largest ones; hence the exponential complexity remains. Nevertheless, with the max-log approximation, one can make any hard decision detector, such as SD, to produce soft values. This has resulted in much of the literature focusing on finding efficient hard decision methods. In this paper, we make a clean break with this philosophy and instead devise a good approximation of the LLRs (4) and (5) directly.

In order to explain our proposed method and the competing state-of-the-art methods, for fixed $n_s \in \{1, \dots, N_T\}$, we define the following partitioning of the model in (1)

$$\mathbf{y} = \mathbf{H}\mathbf{s} + \mathbf{e} = \underbrace{\begin{bmatrix} \bar{\mathbf{H}} & \tilde{\mathbf{H}} \end{bmatrix}}_{\text{col. permut. of } \mathbf{H}} \underbrace{\begin{bmatrix} \bar{\mathbf{s}}^T & \tilde{\mathbf{s}}^T \end{bmatrix}^T}_{\text{permut. of } \mathbf{s}} + \mathbf{e} = \bar{\mathbf{H}}\bar{\mathbf{s}} + \tilde{\mathbf{H}}\tilde{\mathbf{s}} + \mathbf{e}, \quad (7)$$

where $\bar{\mathbf{H}} \in \mathbb{R}^{N_R \times n_s}$, $\tilde{\mathbf{H}} \in \mathbb{R}^{N_R \times (N_T - n_s)}$, $\bar{\mathbf{s}} \in \mathcal{S}^{n_s}$ contains the i th bit s_i in the original vector \mathbf{s} , and $\tilde{\mathbf{s}} \in \mathcal{S}^{N_T - n_s}$. The choice of partitioning involves the choice of a permutation, and how to make this choice (for $n_s > 1$) is not obvious. For each bit in \mathbf{s} , there are $\binom{N_T-1}{n_s-1}$ possible permutations in (7). How we perform this partitioning is explained in Sec. III-C. Note that for different detectors, the choice of partitioning serves different purposes.

B. Today's State-of-the-Art MIMO Detectors

Note that all of the methods explained in this subsection, except for PM, are designed to deliver hard decisions. These methods can then produce soft decisions by using the max-log approximation.

The PM Method: PM [12] offers a tradeoff between exact and approximate computation of (5), via a parameter $r = n_s - 1 \in \{0, \dots, N_T - 1\}$. We present the slightly modified version in [29] of the original method in [12], which is simpler than that in [12] but without comprising performance. The PM method implements a two-step approximation of (5). More specifically, in the first step it approximates the sums of (5) that correspond to $\tilde{\mathbf{s}} \in \mathcal{S}^{N_T - n_s}$ with a maximization,

$$l(s_i|\mathbf{y}) \approx \log \left(\frac{\sum_{\tilde{\mathbf{s}}:s_i(\tilde{\mathbf{s}})=+1} \max_{\tilde{\mathbf{s}}} \exp\left(-\frac{1}{N_0} \|\mathbf{y} - \bar{\mathbf{H}}\tilde{\mathbf{s}} - \tilde{\mathbf{H}}\tilde{\mathbf{s}}\|^2\right)}{\sum_{\tilde{\mathbf{s}}:s_i(\tilde{\mathbf{s}})=-1} \max_{\tilde{\mathbf{s}}} \exp\left(-\frac{1}{N_0} \|\mathbf{y} - \bar{\mathbf{H}}\tilde{\mathbf{s}} - \tilde{\mathbf{H}}\tilde{\mathbf{s}}\|^2\right)} \right). \quad (8)$$

In the second step, the maximization in (8) is approximated with a linear filter with quantization (clipping), such as the zero-forcing with decision-feedback (ZF-DF) detector [12]. The ZF-DF method is computationally much more efficient than exact maximization, but it performs well only for well-conditioned matrices $\bar{\mathbf{H}}$. However, the max problems in (8) are generally well-conditioned since the matrices $\bar{\mathbf{H}}$ are typically tall. For PM, when forming the partitioning in (7), the original bit-order in $\mathbf{s} = [s_1, \dots, s_{N_T}]^T$ is permuted in (8) in a way such that the condition number of $\bar{\mathbf{H}}$ is minimized, see [12]. Notably, PM performs ZF-DF aided max-log detection in the special case of $r = 0$ and computes the exact LLR values (as defined by (5)) for $r = N_T - 1$.

The FCSD Method: As already noted, SD is a well known method for computing hard decisions. All variants of SD have a random complexity (runtime). This is a very undesirable property from a hardware implementation point of view, and this is one of the insights that stimulated the development of the FCSD method [13] (as well as PM [12] and our proposed SUMIS). FCSD performs essentially the same procedure as the PM method except that it introduces an additional approximation by employing max-log on the sums in the PM method, i.e., the sums over $\{\tilde{\mathbf{s}} \in \mathcal{S}^{n_s} : s_i(\tilde{\mathbf{s}}) = x\}$ in (8). Hence, instead of summing over $\{\tilde{\mathbf{s}} \in \mathcal{S}^{n_s} : s_i(\tilde{\mathbf{s}}) = x\}$ for each x as in PM, it picks the best candidate from $\{\tilde{\mathbf{s}} \in \mathcal{S}^{n_s} : s_i(\tilde{\mathbf{s}}) = x\}$ for each x . As a result, the FCSD method offers a tradeoff between exact and approximate computation of the max-log problem in (6).

The SD Method and Its Soft-Output Derivatives: The conventional SD method [30], which also constitutes the core of its many derivatives such as [9], [14], [18], [31]–[33], does not use the partitioned model in (7). It uses a (sorted) QR-decomposition $\mathbf{H} = \mathbf{\Pi}\mathbf{R}$, where $\mathbf{\Pi} \in \mathbb{R}^{N_R \times N_T}$ has orthonormal columns and $\mathbf{R} \in \mathbb{R}^{N_T \times N_T}$ is an upper-triangular matrix, in order to write $\arg\min_{\mathbf{s}:s_i=x} \|\mathbf{y} - \mathbf{H}\mathbf{s}\|^2 = \arg\min_{\mathbf{s}:s_i=x} \|\mathbf{\Pi}^T \mathbf{y} - \mathbf{R}\mathbf{s}\|^2$ for each x so that the max-log problem in (6) can be solved by means of a tree-search. This search requires the choice of an initial sphere radius and success is only guaranteed if the initial radius is large enough and if the search is not prematurely terminated [30]. SD has a high complexity for some channel realizations (the average complexity is known to be exponential in N_T [34]), and hence, in practice a stopping criterion is used to terminate

the algorithm after a given number of operations. Particularly, SD requires more time to finish for ill-conditioned than for well-conditioned channel realizations. To reduce the negative effect of ill-conditioned matrices, matrix regularization [18], [35] or lattice reduction techniques [10] can be applied. The idea of the latter is to apply, after relaxing the boundaries of the signal constellation, a transformation that effectively reduces the condition number of the channel matrix. Using SD to solve (6) naively would require two runs of the procedure per bit, which becomes computationally prohibitive when detecting a vector of bits. We next review some methods that tackle this issue.

In the list sphere-decoder [33], a list of a fixed number of candidates is stored during the search through the tree (one single tree-search is performed). Then (6) is solved approximately by picking out the minimum-norm candidates in the resulting candidate list instead of in the full multi-dimensional constellation. Unfortunately, this procedure does not guarantee that the signal vector candidates with the smallest norms are included in the resulting list and thus performance is compromised. The list size and the sphere radius must be very carefully chosen. A more sophisticated version of this method can be found in [32].

In the repeated tree-search method [31], the tree-search is performed multiple times but not as many times as in the naive approach. In the first run, the algorithm performs one single tree-search that finds the vector with the smallest norm $\arg\min_{\mathbf{s}} \|\mathbf{\Pi}^T \mathbf{y} - \mathbf{R}\mathbf{s}\|^2$. This in effect finds $\arg\min_{\mathbf{s}: s_i=x} \|\mathbf{\Pi}^T \mathbf{y} - \mathbf{R}\mathbf{s}\|^2$ for each bit but only for one of the bit hypotheses (either $x = +1$ or $x = -1$). To find the smallest-norm candidates for the counterhypothesis x^c , a tree-search is performed for each bit to solve $\arg\min_{\mathbf{s}: s_i=x^c} \|\mathbf{\Pi}^T \mathbf{y} - \mathbf{R}\mathbf{s}\|^2$. This method finds the minimums in (6) using only half the number of tree-searches required by the naive approach. In this method, the main disadvantage remains, which is that it may visit the same nodes multiple times.

The single-tree-search method [18], on the other hand, traverses the multiple trees in parallel instead of in a repeated fashion as is done in [31]. While doing that, it keeps track of which nodes have been already visited in one search so that they can be skipped in the rest. That way, this method can guarantee to find the minimums in (6) with one extended single tree-search and hence provides clear advantages over methods in both [33] and [31].

The RD-MLS Method: RD-MLS [9], [14] carries out the same procedure as FCSD except that it does not perform clipping after the linear filtering. Instead, it uses an SD type of algorithm to perform a reduced tree-search over $\{\bar{\mathbf{s}} \in \mathcal{S}^{n_s} : s_i(\bar{\mathbf{s}}) = x\}$ for each x . Although this method reduces the number of layers in the tree, it does not necessarily improve the conditioning of the reduced problem, as the PM and FCSD methods do. This is so due to the unquantized linear filtering operation that in effect results in performing a projection of the original space (column space of \mathbf{H}) onto the orthogonal complement of the column space of $\tilde{\mathbf{H}}$. Therefore, for an ill-conditioned matrix \mathbf{H} , even though RD-MLS searches over a

reduced space (roughly half the original space dimension [14, Sec. V], i.e., $n_s \approx N_T/2$), it is unclear whether the RD-MLS algorithm would visit significantly fewer nodes in the reduced space $\bar{\mathbf{s}}$ than in the original space \mathbf{s} . The reason is that the RD-MLS will suffer from the same problem in the reduced space as the conventional SD would have in the original space, namely the slow reduction in radius and pruning of nodes that are not of interest.

III. PROPOSED SOFT MIMO DETECTOR (SUMIS)

Our proposed method, SUMIS, consists of two main stages. In stage I, a first approximation to the a posteriori probability of each bit s_i is computed. In stage II, these approximate LLRs are used in an interference suppression mechanism, whereafter the LLR values are calculated based on the resulting ‘‘purified’’ model. To keep the exposition simple, we herein first present the basic ideas behind SUMIS for the case that $P(\mathbf{s})$ is uniform. The extension to non-uniform $P(\mathbf{s})$ is treated in Sec. IV. A highly optimized version (which has much lower complexity but sacrifices clarity of exposition) of SUMIS is then presented in App. A. A practical implementation of SUMIS should use the version in App. A.

A. Stage I

We start with the partitioned model in (7)

$$\mathbf{y} = \tilde{\mathbf{H}}\bar{\mathbf{s}} + \underbrace{\tilde{\mathbf{H}}\bar{\mathbf{s}} + \mathbf{e}}_{\text{interference+noise}} \quad (9)$$

and define an approximate model $\bar{\mathbf{y}} \triangleq \tilde{\mathbf{H}}\bar{\mathbf{s}} + \mathbf{n}$ where \mathbf{n} is a Gaussian stochastic vector $\mathcal{N}(\mathbf{0}, \mathbf{Q})$ with $\mathbf{Q} \triangleq \tilde{\mathbf{H}}\tilde{\mathbf{\Psi}}\tilde{\mathbf{H}}^T + \frac{N_0}{2}\mathbf{I}$ and $\tilde{\mathbf{\Psi}}$ is the covariance matrix of $\bar{\mathbf{s}}$. Under the assumption that the symbols are independent, $\tilde{\mathbf{\Psi}}$ is diagonal, and since $P(\mathbf{s})$ is uniform, $\tilde{\mathbf{\Psi}} = \mathbf{I}$. It is important to note that $\bar{\mathbf{y}} = \tilde{\mathbf{H}}\bar{\mathbf{s}} + \mathbf{n}$ is an approximated model of (9), which we will use to approximate the probability density function $p(\mathbf{y}|\bar{\mathbf{s}}) \approx p(\bar{\mathbf{y}}|\bar{\mathbf{s}})|_{\bar{\mathbf{y}}=\mathbf{y}}$. The approximation consists of considering the interfering terms $\tilde{\mathbf{H}}\bar{\mathbf{s}}$ as Gaussian. This is a reasonable approximation since each element in $\tilde{\mathbf{H}}\bar{\mathbf{s}}$ constitutes a sum of variates and thus generally has Gaussian behaviour, especially when the variates are many and independent. This is a consequence of the central limit theorem, see [36, sec. 8.5] and [36, fig. 8.4b].

To compute the a posteriori probability $P(s_k|\mathbf{y})$ of a bit s_k , which is contained in $\bar{\mathbf{s}}$, we can marginalize out the remaining bits in $P(\bar{\mathbf{s}}|\mathbf{y})$. Note that computing $P(\bar{\mathbf{s}}|\mathbf{y})$ itself requires marginalizing out $\bar{\mathbf{s}}$ from $P(\mathbf{s}|\mathbf{y})$, which is computationally very burdensome. However, with our proposed approximation, we can write

$$P(\bar{\mathbf{s}}|\mathbf{y}) \propto p(\mathbf{y}|\bar{\mathbf{s}})P(\bar{\mathbf{s}}) \propto p(\mathbf{y}|\bar{\mathbf{s}}) \approx p(\bar{\mathbf{y}}|\bar{\mathbf{s}})|_{\bar{\mathbf{y}}=\mathbf{y}}, \quad (10)$$

and therefore approximate the a posteriori probability function $P(s_k|\mathbf{y})$ with the function

$$P(s_k = s|\mathbf{y})|_{\bar{\mathbf{y}}=\mathbf{y}} \propto \sum_{\bar{\mathbf{s}}: s_k=s} p(\bar{\mathbf{y}}|\bar{\mathbf{s}})|_{\bar{\mathbf{y}}=\mathbf{y}}. \quad (11)$$

Note that the number of terms in the summation over $\bar{\mathbf{s}} : s_k = s$ is 2^{n_s-1} , which is significantly smaller than the number of terms that need to be added when evaluating $P(s_k|\mathbf{y})$ exactly.

Using the following operator $\|\mathbf{x}\|_Q^2 \triangleq \mathbf{x}^T \mathbf{Q}^{-1} \mathbf{x}$ for some vector $\mathbf{x} \in \mathbb{R}^{N_R}$, we write

$$p(\bar{\mathbf{y}}|\bar{\mathbf{s}}) = \frac{1}{\sqrt{(2\pi)^{N_R} |\mathbf{Q}|}} \exp\left(-\frac{1}{2} \|\bar{\mathbf{y}} - \bar{\mathbf{H}}\bar{\mathbf{s}}\|_Q^2\right) \quad (12)$$

and due to the assumption on \mathcal{S} being BPSK, we can perform the marginalization in (11) in the LLR domain as (after inserting \mathbf{y} in place of $\bar{\mathbf{y}}$ in (12))

$$\lambda_k \triangleq \log \left(\frac{\sum_{\bar{\mathbf{s}}: s_k=+1} \exp\left(-\frac{1}{2} \|\mathbf{y} - \bar{\mathbf{H}}\bar{\mathbf{s}}\|_Q^2\right)}{\sum_{\bar{\mathbf{s}}: s_k=-1} \exp\left(-\frac{1}{2} \|\mathbf{y} - \bar{\mathbf{H}}\bar{\mathbf{s}}\|_Q^2\right)} \right). \quad (13)$$

The summations in (13) can be computed efficiently, with good numerical stability, and using low-resolution fixed-point arithmetics via repeated use of the Jacobian logarithm. The a posteriori probabilities of the remaining elements in \mathbf{s} are approximated analogously to (9)-(13) by simply choosing different partitionings (permutations) of $\bar{\mathbf{H}}$ and \mathbf{s} such that the bit of interest is in $\bar{\mathbf{s}}$. The main purpose of stage I is to reduce the impact of the interfering term $\bar{\mathbf{H}}\bar{\mathbf{s}}$. For this purpose, we compute the conditional expected value of bit s_k approximately using the function $P(s_k = s|\bar{\mathbf{y}})$,

$$\begin{aligned} \mathbb{E}\{s_k|\mathbf{y}\} &\triangleq \sum_{s \in \mathcal{S}} s P(s_k = s|\mathbf{y}) \approx \sum_{s \in \mathcal{S}} s P(s_k = s|\bar{\mathbf{y}}) \Big|_{\bar{\mathbf{y}}=\mathbf{y}} \\ &= \frac{-1}{1 + e^{\lambda_k}} + \frac{1}{1 + e^{-\lambda_k}} = \tanh\left(\frac{\lambda_k}{2}\right). \end{aligned} \quad (14)$$

Stage I is performed for all bits s_k in \mathbf{s} , i.e., $k = 1, \dots, N_T$. For higher-order constellations, this stage would be performed symbol-wise rather than bit-wise as presented above. This is the reason for using the index k in place of index i in the description here. Note that the soft MMSE procedure computes (13) bit-wisely with n_s set to one, i.e., soft MMSE essentially is a special case of SUMIS when $n_s = 1$ and stage II is disabled. One can see this equivalence by fixing $n_s = 1$ and comparing the underlying approximation steps, from the exact LLR calculation, we take prior to (13) with those that soft MMSE takes.

B. Stage II: Purification

For each bit s_i , the interfering vector $\tilde{\mathbf{s}}$ in (9) is suppressed using

$$\mathbf{y}' \triangleq \mathbf{y} - \tilde{\mathbf{H}} \mathbb{E}\{\tilde{\mathbf{s}}|\mathbf{y}\} = \bar{\mathbf{H}}\bar{\mathbf{s}} + \underbrace{\tilde{\mathbf{H}}(\tilde{\mathbf{s}} - \mathbb{E}\{\tilde{\mathbf{s}}|\mathbf{y}\})}_{\text{interference+noise}} + e \approx \bar{\mathbf{H}}\bar{\mathbf{s}} + \mathbf{n}', \quad (15)$$

where $\mathbf{n}' \sim \mathcal{N}(\mathbf{0}, \mathbf{Q}')$ with $\mathbf{Q}' \triangleq \tilde{\mathbf{H}}\tilde{\Phi}\tilde{\mathbf{H}}^T + \frac{N_0}{2}\mathbf{I}$ and $\tilde{\Phi}$ is the conditional covariance matrix of $\tilde{\mathbf{s}}$. Note that it is natural to suppress the interference by subtracting its conditional mean since this removes the bias that the interference causes. Under the approximation that the elements in $\tilde{\mathbf{s}}$ are independent conditioned on \mathbf{y} , we have that

$$\tilde{\Phi} = \mathbb{E}\{\text{diag}(\tilde{\mathbf{s}})^2|\mathbf{y}\} - \mathbb{E}\{\text{diag}(\tilde{\mathbf{s}})|\mathbf{y}\}^2, \quad (16)$$

where the operator $\text{diag}(\cdot)$ takes a vector of elements as input and returns a diagonal matrix with these elements on its diagonal, and the notation \mathbf{A}^2 means $\mathbf{A}\mathbf{A}$ for some square matrix \mathbf{A} . Since $\mathcal{S} = \{-1, +1\}$, we get

$$\tilde{\Phi} = \mathbf{I} - \text{diag}(\mathbb{E}\{\tilde{\mathbf{s}}|\mathbf{y}\})^2. \quad (17)$$

After the interfering vector $\tilde{\mathbf{s}}$ is suppressed and the model is “purified”, we compute the LLRs. The LLRs are computed by performing a full-blown marginalization in (5) over the corresponding n_s -dimensional subspace $\bar{\mathbf{s}}$ using the purified approximate model in (15). Hence, the LLR value we compute for the i th bit is

$$l(s_i|\mathbf{y}) \approx \log \left(\frac{\sum_{\bar{\mathbf{s}}: s_i(\bar{\mathbf{s}})=+1} \exp\left(-\frac{1}{2} \|\mathbf{y}' - \bar{\mathbf{H}}\bar{\mathbf{s}}\|_{Q'}^2\right)}{\sum_{\bar{\mathbf{s}}: s_i(\bar{\mathbf{s}})=-1} \exp\left(-\frac{1}{2} \|\mathbf{y}' - \bar{\mathbf{H}}\bar{\mathbf{s}}\|_{Q'}^2\right)} \right). \quad (18)$$

For higher order constellations, this stage is performed bit-wise; hence we use the index i .

C. Choosing the Permutations

The optimal permutation that determines $\bar{\mathbf{H}}$ and $\tilde{\mathbf{H}}$ would be the one that minimizes the probability of a decoding error. This permutation is hard to find as it is difficult to derive tractable expressions of the probability of decoding error. There are many possible heuristic ways to choose the permutations. For instance, in the PM and FCSD methods, the aim is to find a permutation such that the condition number, i.e., the ratio between the largest and smallest singular values, of $\tilde{\mathbf{H}}$ is minimized. The reason for this choice is that the matrix $\tilde{\mathbf{H}}$ determines the conditioning of the subproblem in PM, which in turn is solved by applying a zero-forcing filter. In SUMIS, by contrast, we aim to choose the partitioning such that for a bit s_k in \mathbf{s} , the interfering vector $\tilde{\mathbf{s}}$ in (9) has as little effect on the useful signal vector $\bar{\mathbf{s}}$ as possible. This in essence means that we would like the interference to lie in the null-space of the useful signal, i.e., the inner product between the columns in $\bar{\mathbf{H}}$ and those in $\tilde{\mathbf{H}}$ should be as small as possible. In the extreme case when the column spaces of $\bar{\mathbf{H}}$ and $\tilde{\mathbf{H}}$ are orthogonal, the marginalization over $\bar{\mathbf{s}}$ and $\tilde{\mathbf{s}}$ decouples and SUMIS would become optimal. In this respect, SUMIS fundamentally differs from PM and FCSD, which instead would become optimal if the permutation could be chosen so that $\tilde{\mathbf{H}}$ had orthogonal columns.

We base our partitioning on $\mathbf{H}^T \mathbf{H}$, which has the structure

$$\mathbf{H}^T \mathbf{H} = \begin{bmatrix} \sigma_1^2 & \rho_{1,2} & \dots \\ \rho_{1,2} & \sigma_2^2 & \\ \vdots & & \ddots \end{bmatrix}. \quad (19)$$

For the k th column of $\mathbf{H}^T \mathbf{H}$ (corresponding to the k th bit in \mathbf{s}) we pick the $n_s - 1$ indices that correspond to the largest values of $|\rho_{k,\ell}|$. Then, these indexes along with the index k specify the columns from \mathbf{H} that are placed in $\bar{\mathbf{H}}$. The rest of the columns are placed in $\tilde{\mathbf{H}}$. Therefore, the choice of permutation will depend on $\bar{\mathbf{H}}^T \bar{\mathbf{H}}$ (the “power” of $\bar{\mathbf{H}}$) and the “correlation” $\bar{\mathbf{H}}^T \tilde{\mathbf{H}}$. Note also that the matrix $\mathbf{H}^T \mathbf{H}$ is used

in the other SUMIS stages and therefore evaluating it here does not add anything to the total computational complexity. Hence, complexity-wise, computing the permutation comes nearly for free. Also, as shown in the numerical results, using the proposed permutation, SUMIS performs close to optimal.

D. Summary

The steps of our SUMIS method are summarized in Alg. 1 in the form of generic pseudo-code. Via the adjustable subspace dimensionality, i.e., the parameter n_s , SUMIS provides a simple and well-defined tradeoff between computational complexity and detection performance. In the special case when $n_s = N_T$, there is no interfering vector \tilde{s} and SUMIS performs exact LLR computation. At the other extreme, if $n_s = 1$ SUMIS becomes the soft MMSE method with the additional step of model purification. The complexity of SUMIS is derived in App. A, and the complexity of some of its competitors is summarized in Tab. 1. The complexity is measured in terms of elementary operations bundled together: additions, subtractions, multiplications, and divisions. Further, it is divided into two parts: one part representing calculations done once for each channel matrix (“ \mathbf{y} -independent”) and one part to be done for each received \mathbf{y} -vector (“ \mathbf{y} -dependent”). We can see that PM requires approximately $(2N_T^3 + 4N_T^2)2^{n_s}$ operations in the \mathbf{y} -dependent part only, and max-log (via SD) requires $3(N_R + N_T)N_T^2$ in the initialization stage only¹. Thus, SUMIS provides clear complexity savings and it does so, as we will see in Sec. VII, at the same time as it offers significant performance gains over these competing methods.

Algorithm 1 SUMIS pseudo-code implementation

```

Start with some  $\mathbf{H}$ ,  $\mathbf{y}$  and  $n_s \in \{1, \dots, N_T\}$ 
for  $k = 1, \dots, N_T$  do // – Stage I – //
    Decide upon a partitioning in (7) based on  $\mathbf{H}^T \mathbf{H}$ 
    Calculate  $\lambda_k$  in (13) (cond. probability of  $s_k$  in terms of LLR)
    Calculate  $\mathbb{E}\{s_k|\mathbf{y}\}$  and  $\text{Var}\{s_k|\mathbf{y}\} = 1 - \mathbb{E}\{s_k|\mathbf{y}\}^2$  in (14)
end for
for each bit in  $\mathbf{s}$  do // – Stage II – //
    Suppress the interfering vector  $\tilde{s}$  and calculate  $\mathbf{y}'$  in (15)

    Calculate the new covariance matrix  $\mathbf{Q}'$ 
    Calculate the LLR in (18)
end for

```

IV. NON-UNIFORM A PRIORI PROBABILITIES

Algorithm 1 in Sec. III can be directly extended to the case of non-uniform $P(s)$. The details for each step are given as follows.

¹The significant initialization complexity of SD is a result of the computation of the sorted QR decomposition [37] on regularized channel models [18], [35]. Channel regularization is used to reduce the impact of ill-conditioned channel matrices on the size of the tree-search. This complexity is much larger compared to the LDL-decomposition, which is used favorably in SUMIS, see App. A.

A. Stage I

Since we have a priori information on the symbols, we can purify the model already in this stage and suppress the interfering subspace \tilde{s} . First, we evaluate the expected value $\mathbb{E}\{s_k\} \triangleq \sum_{s \in \mathcal{S}} sP(s_k = s)$ and the purified received data

$$\mathbf{y} - \tilde{\mathbf{H}}\mathbb{E}\{\tilde{s}\} = \tilde{\mathbf{H}}\tilde{s} + \underbrace{\tilde{\mathbf{H}}(\tilde{s} - \mathbb{E}\{\tilde{s}\})}_{\text{interference+noise}} + \mathbf{e}, \quad (20)$$

where the “interference+noise” is, as in (9) in the approximate model $\tilde{\mathbf{y}} = \tilde{\mathbf{H}}\tilde{s} + \mathbf{n}$, approximated to be $\mathcal{N}(\mathbf{0}, \mathbf{Q})$ where now $\tilde{\Psi}$ in \mathbf{Q} is not necessarily equal to the identity matrix. More precisely, under the restriction that $\mathcal{S} = \{-1, +1\}$ and the assumption that the bits s_k are independent, we get

$$\tilde{\Psi} = \mathbf{I} - \text{diag}(\mathbb{E}\{\tilde{s}\})^2. \quad (21)$$

We can approximate the a posteriori probability $P(s_k = s|\mathbf{y})$, analogously to (11), with

$$P(s_k = s|\mathbf{y}) \propto \sum_{\tilde{s}: s_k = s} p(\tilde{\mathbf{y}}|\tilde{s})P(\tilde{s}). \quad (22)$$

Using (22), we can approximate the expectation of s_k conditioned on \mathbf{y} in the same manner as in (14), i.e.,

$$\mathbb{E}\{s_k|\mathbf{y}\} \approx \tanh\left(\frac{\lambda_k}{2}\right), \quad \lambda_k = \log\left(\frac{P(s_k = +1|\tilde{\mathbf{y}})}{P(s_k = -1|\tilde{\mathbf{y}})}\right)\bigg|_{\tilde{\mathbf{y}}=\mathbf{y}}. \quad (23)$$

Similarly to stage I in Sec. III for higher-order constellations, this stage is performed symbol-wise; hence we use here again the index k . Note that for BPSK constellations, the procedure in [11] is equivalent to stage I here, i.e., the method of [11] is a special case of SUMIS when stage II is disabled.

B. Stage II

In this stage, exactly the same procedure is performed as in stage II in Sec. III but with two minor modifications: first the model is purified using (23) instead of (14), and second, the LLR value of the i th bit is computed using

$$l(s_i|\mathbf{y}) \approx \log\left(\frac{\sum_{\tilde{s}: s_i(\tilde{s})=+1} \exp\left(-\frac{1}{2}\|\mathbf{y}' - \tilde{\mathbf{H}}\tilde{s}\|_{\mathbf{Q}'}^2\right) P(\tilde{s})}{\sum_{\tilde{s}: s_i(\tilde{s})=-1} \exp\left(-\frac{1}{2}\|\mathbf{y}' - \tilde{\mathbf{H}}\tilde{s}\|_{\mathbf{Q}'}^2\right) P(\tilde{s})}\right). \quad (24)$$

For higher order constellations, this stage is performed bit-wise; hence the index i .

V. IMPERFECT CHANNEL STATE INFORMATION

In practice the receiver does not have perfect knowledge about \mathbf{H} . Typically, the receiver then forms an estimate of the channel, based on a known transmitted pilot matrix $\mathbf{s}^{1:N_{\text{TR}}} \triangleq [\mathbf{s}_1 \dots \mathbf{s}_{N_{\text{TR}}}]$ and the corresponding received matrix $\mathbf{y}^{1:N_{\text{TR}}} \triangleq [\mathbf{y}_1 \dots \mathbf{y}_{N_{\text{TR}}}]$. The so-obtained estimated channel matrix will not be perfectly accurate, and the estimation error should be taken into account when computing the LLRs.

To optimally account for the imperfect knowledge of the channel, $P(s|\mathbf{y})$ (or $P(s|\mathbf{y}, \mathbf{H})$) if the dependence

Det. method	\mathbf{y} -independent	\mathbf{y} -dependent
SUMIS (proposed)	$N_R N_T^2 + N_T^3 + 2n_s^2 N_T^2$	$N_T^3 + 2N_R N_T + (2n_s^2 + 6)N_T^2$
SD aided max-log	$3(N_R + N_T)N_T^2$	random and exponential in N_T on average [34]
PM	$N_R N_T^2 + N_T^3$	$(2N_T^3 + 4N_T^2)M^{n_s}$
soft MMSE	$N_R N_T^2 + N_T^3$	$2N_T(N_R + N_T)$
max-log	$3N_T M^{N_T}$	$N_T M^{N_T}$
exact LLR	$3N_T M^{N_T}$	$N_T M^{N_T}$

Tab. 1: Complexity summary in terms of elementary operations bundled together. Here $M \triangleq |\mathcal{S}|$ denotes the cardinality of the constellation. The derivation of the SUMIS complexity is presented in App. A. PM includes initialization (same as for SUMIS) and the computation of $N_T M^{n_s}$ norms required to produce the soft values. Soft MMSE requires a similar initialization (assuming that the matrix inverse is explicitly computed) and two matrix-vector multiplications to compute the required norms. SD-aided max-log includes a sorted QR-decomposition [37] of a regularized channel matrix [18], [35] during the initialization (\mathbf{y} -independent part) and a tree-search of random complexity per \mathbf{y} , see Fig. 5 for an empirical example. For the max-log and exact LLR, we have included the complexity of computing all M^{N_T} norms and then performing the comparisons and summations, respectively. To achieve the presented complexity figures of max-log and exact LLR, we sort the symbol vectors such that each consecutive vector differs only in one element from the previous vector. This facilitates computation of all 2^{N_T} norms via a simple differential update procedure. Note that this table presents the complexity figures of the bottlenecks of each algorithm and are representative for $N_R \geq N_T \gtrsim 10$ and $N_T \gg n_s$ (or $N_T^2 \gg M^{n_s}$ specifically for SUMIS, see App. A2).

on \mathbf{H} is spelled out explicitly) should be replaced with $P(\mathbf{s}|\mathbf{y}, \mathbf{y}^{1:N_{\text{TR}}}, \mathbf{s}^{1:N_{\text{TR}}})$ in (4). As an approximation to the resulting optimal detector, instead of working with $P(\mathbf{s}|\mathbf{y}, \mathbf{y}^{1:N_{\text{TR}}}, \mathbf{s}^{1:N_{\text{TR}}})$, \mathbf{H} may be replaced with an estimate $\hat{\mathbf{H}}$ of \mathbf{H} in $P(\mathbf{s}|\mathbf{y}, \mathbf{H})$. The so-obtained detector is called *mismatched*, and it is generally not optimal, except for in some special cases [38].

We next extend SUMIS to take into account channel estimation errors, i.e., using $P(\mathbf{s}|\mathbf{y}, \mathbf{y}^{1:N_{\text{TR}}}, \mathbf{s}^{1:N_{\text{TR}}})$ in (4). We model the channel estimate $\hat{\mathbf{H}}$, when obtained using the training data $\mathbf{s}^{1:N_{\text{TR}}}$ and $\mathbf{y}^{1:N_{\text{TR}}}$, with

$$\hat{\mathbf{H}} = \mathbf{H} + \mathbf{\Delta}, \quad (25)$$

where \mathbf{H} is the true channel and $\mathbf{\Delta}$ is the estimation error matrix whose complex-valued counterpart $\mathbf{\Delta}_c$ (which is decomposed into $\mathbf{\Delta}$ using (3)) has independent $\mathcal{CN}(0, \delta^2)$ elements where δ^2 is the variance of the estimation error per complex dimension. Typically, δ^2 is directly proportional to the noise variance N_0 . The assumption that the elements in $\mathbf{\Delta}$ are independent holds if the pilots are orthogonal and the noise is uncorrelated. Further, we assume that the elements in $\hat{\mathbf{H}}$ are independent of those in $\mathbf{\Delta}$; this is the case if MMSE channel estimation is used [39]. From (1) and (25), we have

$$\mathbf{y} = \mathbf{H}\mathbf{s} + \mathbf{e} = \hat{\mathbf{H}}\mathbf{s} + \underbrace{\mathbf{e} - \mathbf{\Delta}\mathbf{s}}_{\triangleq \boldsymbol{\epsilon}} = \hat{\mathbf{H}}\mathbf{s} + \boldsymbol{\epsilon}. \quad (26)$$

For constellations that have constant modulus, i.e., satisfy $\|\mathbf{s}\|^2 = N_T \forall \mathbf{s}$, we know that $\boldsymbol{\epsilon} \sim \mathcal{N}(0, \frac{N_T \delta^2 + N_0}{2} \mathbf{I})$. In this case, SUMIS can be directly applied to a modified data model where $\hat{\mathbf{H}}$ and $\boldsymbol{\epsilon}$ are the channel matrix and noise vector, respectively.

By contrast, for general signal constellations, $\|\mathbf{s}\|^2$ is not equal to a constant, and the situation becomes more compli-

cated. Recall that $P(\mathbf{s}|\mathbf{y}, \hat{\mathbf{H}}) = p(\mathbf{y}|\mathbf{s}, \hat{\mathbf{H}})P(\mathbf{s})/p(\mathbf{y})$, where the goal is to approximate $p(\mathbf{y}|\mathbf{s}, \hat{\mathbf{H}})$ via $p(\mathbf{y}|\bar{\mathbf{s}}, \hat{\mathbf{H}})$ using the philosophy of SUMIS. That is, we target $p(\mathbf{y}|\bar{\mathbf{s}}, \hat{\mathbf{H}})$ by approximating $\boldsymbol{\epsilon}$ conditioned on $\bar{\mathbf{s}}$ and $\hat{\mathbf{H}}$ as Gaussian. Approximating $\boldsymbol{\epsilon}|\bar{\mathbf{s}}, \hat{\mathbf{H}}$ as Gaussian is reasonable since each element in $\boldsymbol{\epsilon}$ consists of a sum of independent variates. The covariance matrix of $\boldsymbol{\epsilon}$ conditioned on $\bar{\mathbf{s}}$ and $\hat{\mathbf{H}}$ is $\frac{(\mathbb{E}\{\|\bar{\mathbf{s}}\|^2\} + \|\bar{\mathbf{s}}\|^2)\delta^2 + N_0}{2} \mathbf{I}$. Thus, the power of the effective noise is $\frac{(\mathbb{E}\{\|\bar{\mathbf{s}}\|^2\} + \|\bar{\mathbf{s}}\|^2)\delta^2 + N_0}{2}$ instead of $\frac{N_0}{2}$ as in Sec. III. This power now depends on $\mathbb{E}\{\|\bar{\mathbf{s}}\|^2\}$ and $\bar{\mathbf{s}}$, causing the complexity of SUMIS to increase substantially. The reason is that the inverse of \mathbf{Q} must be recomputed for each permutation in (7) and even more often for each $\bar{\mathbf{s}}$; the same applies in stage II of SUMIS for the \mathbf{Q}' matrix.

To avoid this complexity increase, we introduce further approximations. First, instead of $\mathbb{E}\{\|\bar{\mathbf{s}}\|^2\}$, we use

$$\eta \triangleq \sum_{\substack{\text{all } N_T \\ \text{permut.}}} \frac{1}{N_T} \mathbb{E}\{\|\bar{\mathbf{s}}\|^2\}, \quad (27)$$

where the sum is taken over all N_T permutations considered in SUMIS for a particular \mathbf{H} . This is reasonable since $N_T \gg n_s$ and at most n_s elements out of $N_T - n_s$ in $\bar{\mathbf{s}}$ are replaced from one permutation to another; hence, $\mathbb{E}\{\|\bar{\mathbf{s}}\|^2\}$ will not differ much over the permutations. Second, using again that $N_T \gg n_s$, the variations in $\|\bar{\mathbf{s}}\|^2$ will have a minor effect on the absolute power of the effective noise. Therefore, we replace $\|\bar{\mathbf{s}}\|^2$ by $\frac{1}{|\mathcal{S}|^{n_s}} \sum_{\bar{\mathbf{s}} \in \mathcal{S}^{n_s}} \|\bar{\mathbf{s}}\|^2 = n_s$. Hence, the simplified noise power becomes $\frac{(\eta + n_s)\delta^2 + N_0}{2}$, which is constant for each stage and results in a SUMIS complexity equivalent to that of the full CSI approach, i.e., the complexity presented in App. A.

VI. VERY LARGE MIMO SETTINGS

SUMIS was developed mainly for moderately-sized MIMO systems but it is also applicable to large MIMO channels. Previous research on detection in MIMO systems with a large number of transmit antennas has focused on hard decision algorithms [3], [5]–[7]. The performance of such algorithms when used in coded systems is always upper-bounded by the performance of max-log. In some cases (see the numerical results in Sec. VII), the performance loss of the max-log approximation becomes larger when the number of antennas increases. Hence, the philosophy behind SUMIS—to approximate the LLR directly—seems to be beneficial.

Another interesting observation in the large-MIMO setting is that even the soft MMSE method can potentially achieve the performance of the exact LLR method and thus outperform the max-log method. This observation is motivated by the central limit theorem and the following argument. Consider the model in (7) for $n_s = 1$, which makes $\tilde{\mathbf{H}}$ a column vector, say \mathbf{h}_i , and $\tilde{\mathbf{s}}$ a scalar, say s_i ; hence, $\mathbf{y} = \mathbf{h}_i s_i + \tilde{\mathbf{H}} \tilde{\mathbf{s}} + \mathbf{e}$. We assume that the elements in \mathbf{s} are independent, which is a very common assumption in the literature and a very reasonable assumption in practice as the bits in a codeword are typically interleaved. By the central limit theorem, the distribution of \mathbf{y} for a given s_i will approach a Gaussian: $\mathcal{N}(\mathbf{h}_i s_i, \tilde{\mathbf{H}} \tilde{\Psi} \tilde{\mathbf{H}}^T + \frac{N_0}{2} \mathbf{I})$, as N_T grows [36, sec. 8.5]. The exact LLR, i.e., $L(s_i|\mathbf{y}) = \log(p(\mathbf{y}|s_i = +1)) - \log(p(\mathbf{y}|s_i = -1))$, will then for sufficiently large N_T look like the LLR function based on the Gaussian distribution, i.e.,

$$L(s_i|\mathbf{y}) \approx 4\mathbf{y}^T (\tilde{\mathbf{H}} \tilde{\Psi} \tilde{\mathbf{H}}^T + \frac{N_0}{2} \mathbf{I})^{-1} \mathbf{h}_i, \quad \text{for } N_T \gg 1. \quad (28)$$

This is a simple but important observation which does not seem to have been made in the existing literature on large-MIMO detection [2]–[7]. However, the question remains as to how large N_T needs to be for the approximation in (28) to be tight. According to [36, sec. 8.5], under some conditions, the approximation becomes very tight even for small values of N_T . We are particularly interested in determining how tight it is in terms of frame-error rate for large but finite N_T . Our investigation with $N_T = 12$ and $N_T = 26$ indicates that the performance of the soft MMSE method is much closer to that of the exact LLR method for larger N_T . What is especially interesting for the SUMIS method is that the performance gap between the soft MMSE method and the exact LLR method is reduced remarkably via the procedure in stage II of SUMIS. Recall that the SUMIS method performs the soft MMSE procedure in stage I when $n_s = 1$.

VII. NUMERICAL RESULTS

A. Simulation Setup

Using Monte Carlo simulations we evaluate the performance of SUMIS and compare it to the performance of some competitors. Performance is quantified in terms of frame-error rate (FER) as a function of the normalized signal-to-noise ratio E_b/N_0 where E_b is the total transmitted energy per information bit. To make the results statistically reliable, we count 300 frame errors for each simulated point. We simulate 6×6

and 13×13 complex MIMO systems with M^2 -QAM where $M \in \{2, 4\}$, which means that the detection is performed on equivalent real-valued 12×12 and 26×26 MIMO systems with 2-PAM and 4-PAM modulation. The channel is Rayleigh fading where each complex-valued channel matrix element is independently drawn from $\mathcal{CN}(0, 1)$. We use three different highly optimized irregular low-density parity-check (LDPC) codes with rates $\{2/9, 1/2, 5/6\}$ (note that $2/9 \lesssim 1/4$), each having a codeword length of approximately 10000 bits. We use the parameters of [40] for rate 1/4 and [41], [42] for rate 1/2. For rate 5/6, we use the technique in [43] to generate the code parameters. For more details, see the uploaded supplementary material to this article. Two different coherence times are used: slow fading (each codeword sees one channel realization) and fast fading (each codeword spans 40 channel matrices), respectively. We plot the FER curves of the exact LLR (as defined by (5)), the max-log approximation (6), SUMIS for $n_s = 1, 3$, SUMIS stage-I-only (without the purification procedure) for $n_s = 1, 3$, and PM for $n_s = r + 1 = 3$ [12]. We include the approximate LLRs computed in stage I of SUMIS in order to show the performance gain of the purification step (stage II) of SUMIS. Recall that SUMIS stage-I-only, for $n_s = 1$, is equivalent to the soft MMSE method. For reasons of numerical stability and efficiency, all log-of-sums-of-exponentials were evaluated via repeated use of the Jacobian logarithm. The convention used in the figures that follow is that dashed lines represent the proposed methods and the solid lines represent the competing ones.

Since the FCSD method is an approximation of the PM method, we refrain from plotting its performance curves. We also omit performance plots of RD-MLS and all other SD-based methods due to the fact that they approximate the max-log method, and thus they cannot perform better. Also, the complexity of the initialization step of these algorithms alone is higher than the complexity of the complete SUMIS procedure, see Tab. 1. Moreover, their complexity depends on the channel realization and they have a very high complexity for some channel realizations (the average complexity is exponential in N_T [34]). Taken together, this renders performance-complexity comparisons with SD-based methods less interesting. We have included the max-log curve as a universal indicator of the performance that can be achieved by any SD-type detector.

B. Results

In Fig. 1 we show results for a slow-fading 6×6 MIMO system using 4-QAM modulation and the LDPC code of rate 1/2. There is no iteration between the detector and the decoder, and the transmitted symbols are assumed by the detector to be uniformly distributed. This plot illustrates our principal comparison and the rest (Figs. 2–8) illustrate extended comparisons that deal with different scenarios of interest: slow-/fast-fading, moderate-/large-size MIMO, low-/high-rate codes, full/partial CSI, higher-order constellations, and iterative/non-iterative receivers. Fig. 1 includes all the above mentioned detection methods whereas the remaining figures include only those methods that show noteworthy variations from what is already seen in Fig. 1.

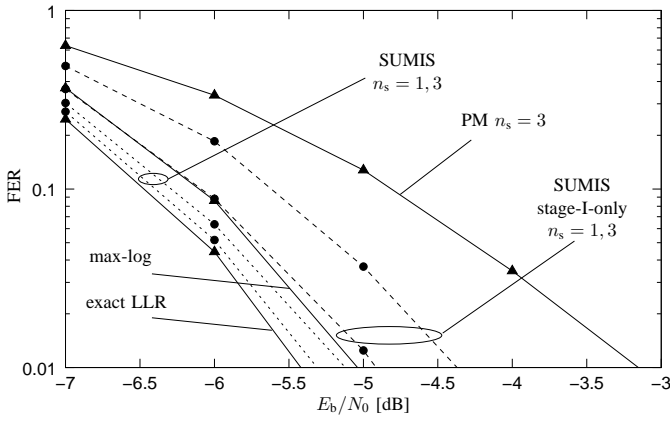


Fig. 1: FER as a function of E_b/N_0 for the slow-fading 6×6 MIMO system ($N_R = N_T = 12$ in (1)) with 4-QAM (2-PAM in (1)) and with the LDPC code of rate $1/2$. The shown performance curves are: (i) dashed curves for the SUMIS stage-I-only and the complete SUMIS procedure with $n_s = 1$ and $n_s = 3$ spanning from right to left, and (ii) solid curves for the exact LLR method, the max-log method, and the PM method with $n_s = r + 1 = 3$.

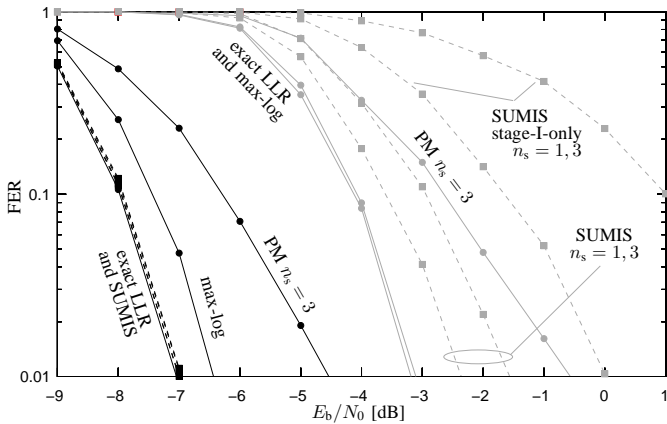


Fig. 2: Same as in Fig. 1 but with LDPC codes of **rate $2/9 \lesssim 1/4$ (black curves)** and **rate $5/6$ (gray curves)**. Note that the left-most blended curves are five different curves: exact LLR, SUMIS for $n_s = 1, 3$, and SUMIS stage-I-only for $n_s = 1, 3$.

The results in Fig. 1 clearly show that the SUMIS detector performs close to the exact LLR (optimal soft detector) performance and it does so at a very low complexity, see also Tab. 1. It outperforms the PM and max-log methods (SD and its derivatives). Note that the complexity of SUMIS with $n_s = 3$ is much lower than that of PM with $n_s = r + 1 = 3$ even though the partitioned problem in (7) is of the same size. The reason is that the sums of the PM method consists of terms whose exponents require the evaluation of matrix-vector multiplications of much larger dimension than in SUMIS. Additionally, SUMIS (both the complete algorithm and the stage-I-only variant) offers a well-defined performance-complexity tradeoff via the choice of the parameter n_s .

Fig. 2 shows results for the same setup as in Fig. 1 but with code rates $2/9 \lesssim 1/4$ and $5/6$ instead. This plot suggest

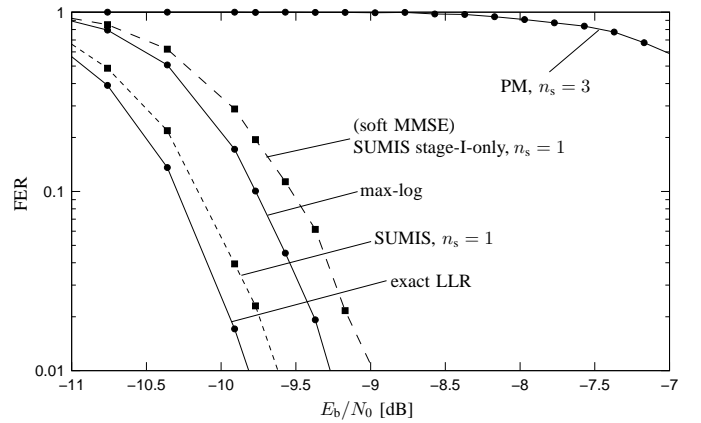


Fig. 3: Same as in Fig. 1 but for a 13×13 MIMO system instead of 6×6 . Note (in contrast to Fig. 1) the increased gap between max-log and exact LLR, and the decreased gap between soft MMSE (SUMIS stage-I-only for $n_s = 1$) and exact LLR. The SUMIS curve is very close to the exact LLR curve.

that there is a larger, but still very small, performance gap between SUMIS and exact LLR for higher coding rates. Also, the max-log curve is much closer to the exact LLR curve for higher rates than for lower rates. The high-rate scenario clearly shows the importance of the model “purification” procedure (SUMIS stage II) as the performance gap between SUMIS and stage-I-only SUMIS is significant. For the low-rate scenario, the performance gap between SUMIS and exact LLR is negligible. Similar results have been observed for short convolution codes with a codeword length of 100 bits, but these plots are not included here due to space limitations. We have also conducted similar experiments with correlated MIMO channels (using a Toeplitz correlation structure) [44], but these results are omitted here due to space limitations. In these experiments, although there was a shift in the absolute performance of all methods, their relative performance, except for that of PM which became much worse, did not differ significantly from what is observed in Figs. 1 and 2. One reason why PM performed differently may be its sensitivity to the condition number of $\tilde{\mathbf{H}}$, which in the correlated MIMO setting is typically much higher than in the uncorrelated case. This stands in contrast to SUMIS which is much more robust in such cases.

A large MIMO system is simulated in Fig. 3. The setup is the same as in Fig. 1 except that here the size of the system is 13×13 complex-valued (corresponding to 26×26 real-valued MIMO). This figure illustrates how close both the soft MMSE (SUMIS stage-I-only with $n_s = 1$) and SUMIS are to the exact LLR performance curve. Plots that include the exact LLR curve for large MIMO systems are unavailable in the literature to our knowledge, probably because of the required enormous simulation time. We used a highly optimized version of the exact LLR detector and it took approximately 50000 core-hours to generate the curves in Fig. 3. A very interesting observation is that in Fig. 3, the gap between the max-log curve and the exact LLR curve is larger than in Fig. 1. This

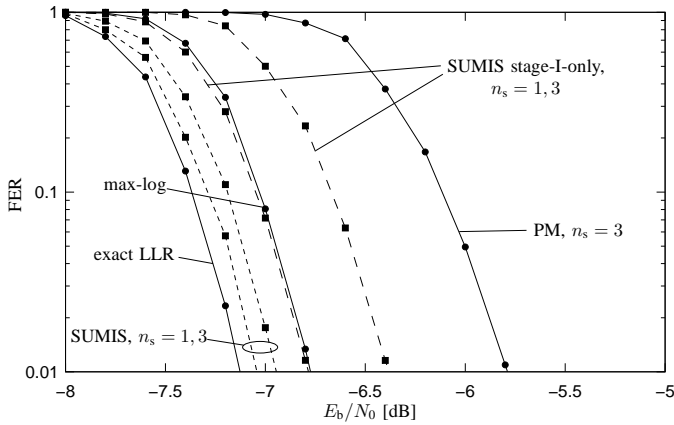


Fig. 4: Same as in Fig. 1 but with fast-fading, i.e., a codeword spans 40 independent channel realizations.

curve represents the performance that the various tree-search algorithms, such as SD with its variants and the method in [3] (which is specifically designed for large MIMO systems), aim to achieve. As predicted in Sec. VI, we see in Fig. 3 that the soft MMSE is much closer to the exact LLR curve than in Fig. 1. Also, the purification step in SUMIS yields a clear compensation for the performance loss of soft MMSE. The performance of SUMIS is impressive, both with stage-I-only and with stage II included, which suggests that approximating the exact LLR expression directly (which is the philosophy of SUMIS) is a better approach than max-log.

Figs. 4 and 5 show the results for a fast-fading scenario. The setup is the same as in Fig. 1, except that here each codeword spans over 40 channel realizations. In Fig. 4, as expected, the relative performance of simple soft MMSE (SUMIS stage-I-only for $n_s = 1$) is much better than in Fig. 1 where the channel stays constant over a whole codeword. The reason is that the presence of ill-conditioned channel matrices, which make linear methods such as soft MMSE and soft ZF perform poorly, has less impact here. With coding over many channel realizations, only a small part of each codeword will be affected by ill-conditioned channel matrices since in i.i.d. Rayleigh fading, they do not occur often (assuming that the MIMO channel is not overly underdetermined). The axes in Fig. 5 show the number of elementary operations bundled together (additions, subtractions, multiplications, and divisions) versus the minimum signal-to-noise ratio required to achieve 1% FER. The values on the horizontal axis are calculated for all methods, except for max-log via SD, using the expressions in Tab. 1. For max-log via SD, the minimum, maximum, and mean complexities of the \mathbf{y} -dependent part were calculated empirically over many different (and random) channel and noise realizations. More specifically, this was done for the single-tree-search algorithm [18] by calculating the number of visited nodes at different tree levels and the associated number of elementary operations at each node (disregarding the overhead of the book-keeping and the “if-and-else” statements). This method, as presented in [18], has k additions/subtractions and k multiplications in each node at tree level k , where the root node is at level 1. The numbers in

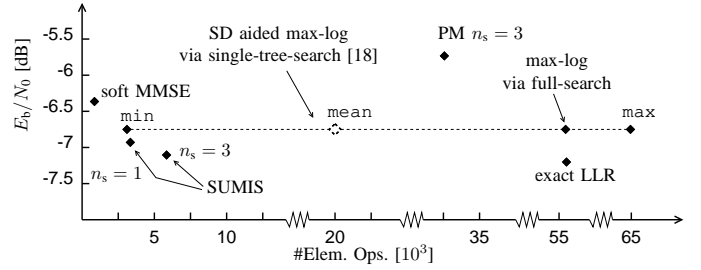


Fig. 5: Total complexity (both \mathbf{y} -independent and \mathbf{y} -dependent parts) per vector of bits in \mathbf{s} for the setting in Fig. 4. In this setting, the channel stays the same for 21 consecutive transmissions of \mathbf{s} . The axes show the number of elementary operations versus the minimum signal-to-noise ratio required to achieve 1% FER. For max-log via SD, we show the empirically evaluated minimum, maximum, and mean complexities.

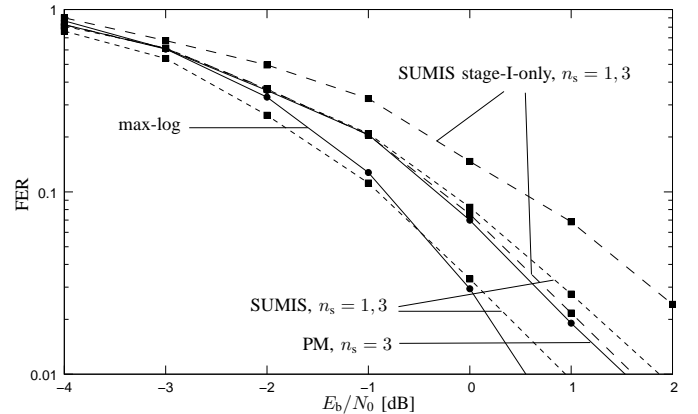
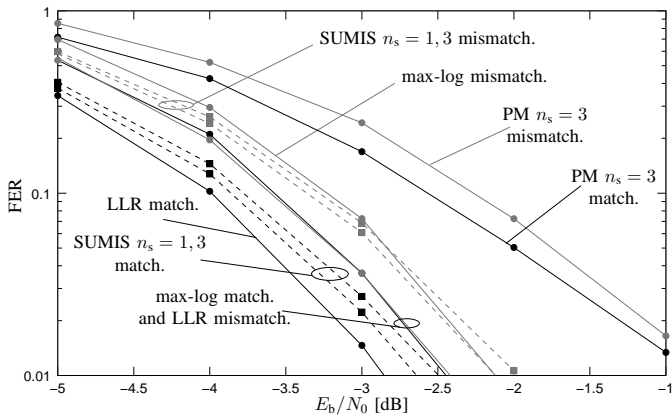


Fig. 6: Same as in Fig. 1 but for 16-QAM (4-PAM in (1)) instead of 4-QAM. The exact LLR curve has been excluded due to the massive complexity required to evaluate the FER. Its complexity is of the same order of magnitude as that in Fig. 3.

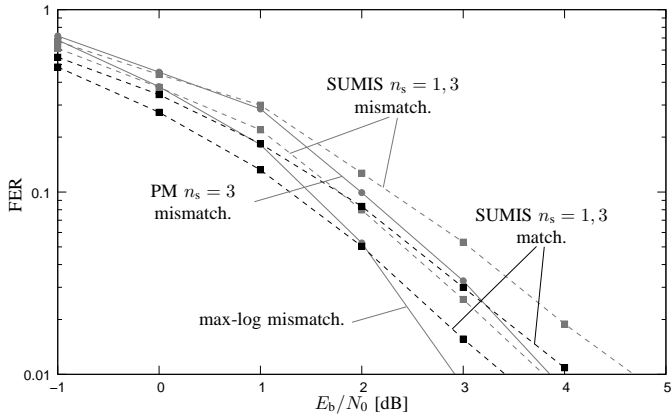
Fig. 5 particularly show the advantages of SUMIS and linear like methods such as soft MMSE.

Fig. 6 reports results with 16-QAM modulation (instead of 4-QAM as used earlier). Except for the modulation, all other parameters are the same as in Fig. 1. The results in Fig. 6 show that the performance of SUMIS is very good and especially in relation to its complexity. For instance, for the \mathbf{y} -dependent part in Tab. 1 (having set $n_s = 3$), SUMIS, PM, and exact LLR require roughly $5.4 \cdot 10^3$, $2.6 \cdot 10^5$, and $2 \cdot 10^8$ operations, respectively. This suggests that the speedup of SUMIS is 50 and $4 \cdot 10^4$ relative to PM and to exact LLR calculation, respectively.

Yet another important scenario that often occurs in practice is detection under imperfect CSI (ICSI). Figs. 7a and 7b presents performance results for this case. The setup is the same as in Fig. 1 and Fig. 6, respectively, but here the detector is provided with knowledge of $\hat{\mathbf{H}}$ instead of \mathbf{H} . The error-matrix-element variance δ^2 is proportional to the noise variance N_0 , i.e., $\delta^2 = \alpha N_0$ where α is a constant. For SUMIS, we considered both the intelligent way of handling



(a) Same as Fig. 1 but with imperfect CSI. The matched SUMIS version used here is the one presented in Sec. V for constant-modulus constellations.



(b) Same as Fig. 6 but with imperfect CSI. The matched SUMIS version used here is presented in Sec. V for non-constant-modulus constellations.

Fig. 7: An example with imperfect CSI at the receiver. The error-matrix-element variance δ^2 is directly proportional to the noise variance N_0 . The matched detectors use $P(s|\mathbf{y}, \hat{\mathbf{H}})$ and the mismatched use $P(s|\mathbf{y}, \mathbf{H})|_{\mathbf{H}=\hat{\mathbf{H}}}$.

ICSI (using $P(s|\mathbf{y}, \hat{\mathbf{H}})$) and the crude way using mismatched detection (inserting $\hat{\mathbf{H}}$ into $P(s|\mathbf{y}, \mathbf{H})$), see Sec. V. For the other detectors, we considered only the mismatched detector since versions of those algorithms that perform intelligent detection using $P(s|\mathbf{y}, \hat{\mathbf{H}})$ and higher-order constellations do not seem to be available. Clearly, intelligently handling ICSI yields better performance than performing mismatched detection. The results in Fig. 7a resemble those in Fig. 1 with only a minor shift in signal-to-noise ratio. This comes as no surprise as the effective channel model in (26) for BPSK per real dimension (as in Fig. 7a) is equivalent to (1) (as in Fig. 1) up to a scaling of the noise variance.

Finally, Fig. 8 shows results with iterative decoding where the detector and the decoder interchange information, hence exploiting the soft-input capability of SUMIS. The iterative decoding setup is that of [23, fig. 1], and the simulation model is the same as used in Fig. 1. SUMIS, as presented in Sec. IV, shows strikingly good performance at very low complexity.

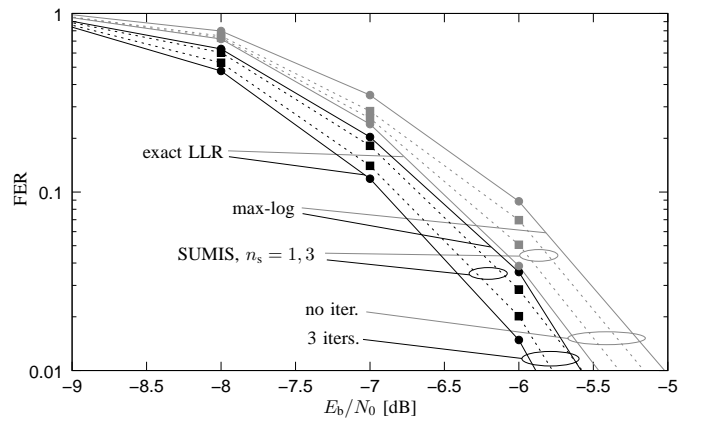


Fig. 8: Detection with iterative decoding using the same setting as in Fig. 1. The curves marked with gray were simulated with no iteration between the respective detector and the outer decoder. For curves marked with black, 3 iterations were used, which means 4 decoder runs. The extended SUMIS algorithm used here is presented in Sec. IV.

VIII. CONCLUSIONS

We have proposed a novel soft-input soft-output MIMO detection method, SUMIS, that outperforms today's state-of-the-art detectors (such as PM, FCSD, SD and its derivatives), runs at fixed-complexity, provides a clear and well-defined tradeoff between computational complexity and detection performance, and is highly parallelizable. The ideas behind SUMIS are fundamentally simple and allow for very simple algorithmic implementations. The proposed method has a complexity comparable to that of linear detectors. We have conducted a thorough numerical performance evaluation of our proposed method and compared to state-of-the-art methods. The results indicate that in many cases SUMIS (for low n_s) outperforms the max-log method and therefore inherently all other methods that approximate max-log, such as SD and its derivatives. This performance is achieved with a complexity that is much smaller than that of competing methods, see Tab. 1 and Fig. 5, and in particular smaller than the initialization step of SD alone. In terms of hardware implementation, SUMIS has remarkable advantages over tree-search (e.g., SD) algorithms that require comparisons and branchings (if-then-else statements).

More fundamentally, the results indicate that approximating the exact LLR expression directly (which is the basic philosophy of SUMIS) is a better approach than max-log followed by hard-decisions. This way of thinking, similar to [12], represents a profound shift in the way the problem is tackled and opens the door for further new approaches to the detection problem. The increase in performance that this philosophy offers is especially pronounced in larger MIMO systems where the performance gap between the max-log approximation and the exact LLR seems to increase.

$$\begin{aligned}
\|\bar{\mathbf{y}} - \bar{\mathbf{H}}\bar{\mathbf{s}}\|_Q^2 &= (\bar{\mathbf{y}} - \bar{\mathbf{H}}\bar{\mathbf{s}})^T \mathbf{Q}^{-1} (\bar{\mathbf{y}} - \bar{\mathbf{H}}\bar{\mathbf{s}}) = \bar{\mathbf{y}}^T \mathbf{Q}^{-1} \bar{\mathbf{y}} - 2\bar{\mathbf{y}}^T \mathbf{Q}^{-1} \bar{\mathbf{H}}\bar{\mathbf{s}} + \bar{\mathbf{s}}^T \bar{\mathbf{H}}^T \mathbf{Q}^{-1} \bar{\mathbf{H}}\bar{\mathbf{s}} \\
&= ((\bar{\mathbf{H}}^T \mathbf{Q}^{-1} \bar{\mathbf{H}})^{-1} \bar{\mathbf{H}}^T \mathbf{Q}^{-1} \bar{\mathbf{y}} - \bar{\mathbf{s}})^T \bar{\mathbf{H}}^T \mathbf{Q}^{-1} \bar{\mathbf{H}} ((\bar{\mathbf{H}}^T \mathbf{Q}^{-1} \bar{\mathbf{H}})^{-1} \bar{\mathbf{H}}^T \mathbf{Q}^{-1} \bar{\mathbf{y}} - \bar{\mathbf{s}}) \\
&\quad + \bar{\mathbf{y}}^T \mathbf{Q}^{-1} \bar{\mathbf{y}} - \bar{\mathbf{y}}^T \mathbf{Q}^{-1} \bar{\mathbf{H}} (\bar{\mathbf{H}}^T \mathbf{Q}^{-1} \bar{\mathbf{H}})^{-1} \bar{\mathbf{H}}^T \mathbf{Q}^{-1} \bar{\mathbf{y}}
\end{aligned} \tag{29}$$

$$\begin{aligned}
\bar{\mathbf{H}}^T \mathbf{Q}^{-1} &= \bar{\mathbf{H}}^T \left(\frac{N_0}{2} \mathbf{I} + \tilde{\mathbf{H}} \tilde{\Psi} \tilde{\mathbf{H}}^T \right)^{-1} = \tilde{\Psi}^{-1} \tilde{\Psi} \bar{\mathbf{H}}^T \left(\frac{N_0}{2} \mathbf{I} + \tilde{\mathbf{H}} \tilde{\Psi} \tilde{\mathbf{H}}^T \right)^{-1} \\
&= \tilde{\Psi}^{-1} \tilde{\Psi} \bar{\mathbf{H}}^T \underbrace{\left(\frac{N_0}{2} \mathbf{I} + \mathbf{H} \Psi \mathbf{H}^T - \bar{\mathbf{H}} \tilde{\Psi} \bar{\mathbf{H}}^T \right)^{-1}}_{\text{apply matrix inversion lemma}} \\
&= \tilde{\Psi}^{-1} (\tilde{\Psi}^{-1} - \bar{\mathbf{H}}^T \left(\frac{N_0}{2} \mathbf{I} + \mathbf{H} \Psi \mathbf{H}^T \right)^{-1} \bar{\mathbf{H}})^{-1} \bar{\mathbf{H}}^T \left(\frac{N_0}{2} \mathbf{I} + \mathbf{H} \Psi \mathbf{H}^T \right)^{-1} \\
&= (\mathbf{I} - \bar{\mathbf{H}}^T \left(\frac{N_0}{2} \mathbf{I} + \mathbf{H} \Psi \mathbf{H}^T \right)^{-1} \bar{\mathbf{H}} \tilde{\Psi})^{-1} \bar{\mathbf{H}}^T \left(\frac{N_0}{2} \mathbf{I} + \mathbf{H} \Psi \mathbf{H}^T \right)^{-1}
\end{aligned} \tag{30a}$$

$$\begin{aligned}
\bar{\mathbf{H}}^T \mathbf{Q}^{-1} \bar{\mathbf{H}} &\stackrel{(30a)}{=} (\mathbf{I} - \bar{\mathbf{H}}^T \left(\frac{N_0}{2} \mathbf{I} + \mathbf{H} \Psi \mathbf{H}^T \right)^{-1} \bar{\mathbf{H}} \tilde{\Psi})^{-1} \bar{\mathbf{H}}^T \left(\frac{N_0}{2} \mathbf{I} + \mathbf{H} \Psi \mathbf{H}^T \right)^{-1} \bar{\mathbf{H}} = \\
&\quad \left((\bar{\mathbf{H}}^T \left(\frac{N_0}{2} \mathbf{I} + \mathbf{H} \Psi \mathbf{H}^T \right)^{-1} \bar{\mathbf{H}})^{-1} - \tilde{\Psi} \right)^{-1}
\end{aligned} \tag{30b}$$

$$(\bar{\mathbf{H}}^T \mathbf{Q}^{-1} \bar{\mathbf{H}})^{-1} \bar{\mathbf{H}}^T \mathbf{Q}^{-1} \stackrel{(30)}{=} (\bar{\mathbf{H}}^T \left(\frac{N_0}{2} \mathbf{I} + \mathbf{H} \Psi \mathbf{H}^T \right)^{-1} \bar{\mathbf{H}})^{-1} \bar{\mathbf{H}}^T \left(\frac{N_0}{2} \mathbf{I} + \mathbf{H} \Psi \mathbf{H}^T \right)^{-1} \tag{31a}$$

$$\begin{aligned}
\bar{\mathbf{H}}^T \left(\frac{N_0}{2} \mathbf{I} + \mathbf{H} \Psi \mathbf{H}^T \right)^{-1} &= \bar{\mathbf{P}}^T \mathbf{H}^T \left(\frac{N_0}{2} \mathbf{I} + \mathbf{H} \Psi \mathbf{H}^T \right)^{-1} = \bar{\mathbf{P}}^T \tilde{\Psi}^{-1} \underbrace{\Psi \mathbf{H}^T \left(\frac{N_0}{2} \mathbf{I} + \mathbf{H} \Psi \mathbf{H}^T \right)^{-1}}_{\text{apply matrix inversion lemma}} \\
&= \bar{\mathbf{P}}^T \tilde{\Psi}^{-1} \left(\frac{N_0}{2} \tilde{\Psi}^{-1} + \mathbf{H}^T \mathbf{H} \right)^{-1} \mathbf{H}^T
\end{aligned} \tag{31b}$$

APPENDIX

A. Optimized SUMIS and Soft MMSE and Their Complexity

We first identify the main complexity bottlenecks of SUMIS step by step and keep track of the largest order of magnitude terms. The focus will be on Alg. 1 in Sec. III, its optimization and the number of operations required for its execution. Note that the techniques presented in what follows can also be used for an optimized implementation of the soft MMSE method [45]. The complexity will be measured in terms of elementary operations bundled together: additions, subtractions, multiplications, and divisions. The complexity count is divided into two parts: a received data independent (\mathbf{y} -independent) processing part and an \mathbf{y} -dependent processing part. We will also assume that $n_s \ll N_T \leq N_R$, which is the case of most practical interest. The assumption on $N_T \leq N_R$ is required only for the presented optimized SUMIS version, due to the requirement for various inverses to exist, but analogous complexity reductions can be made for $N_T \geq N_R$ and are excluded due to space limitations.

1) *\mathbf{y} -independent processing*: We start with the choice of permutations in Sec. III-C. The SUMIS algorithm uses N_T different permutations that are decided based on $\mathbf{H}^T \mathbf{H}$. This procedure evaluates $\mathbf{H}^T \mathbf{H}$ requiring $N_T^2 N_R$ operations. There is also a small search involved that requires $N_T(n_s - 1)(N_T - n_s)$ comparisons and this we neglect.

Next, by simple matrix manipulations, one can pre-process and simplify the computation of (11), in the \mathbf{y} -dependent part

of the algorithm, consisting of a sum of terms in (12) over all $\bar{\mathbf{s}}$. Consider again (12),

$$p(\bar{\mathbf{y}}|\bar{\mathbf{s}}) = \frac{1}{\sqrt{(2\pi)^{N_R} |\mathbf{Q}|}} \exp\left(-\frac{1}{2} \|\bar{\mathbf{y}} - \bar{\mathbf{H}}\bar{\mathbf{s}}\|_Q^2\right), \tag{32}$$

which includes matrix-vector multiplications of dimension N_R . We can rewrite the exponent as in (29) where the terms on the last line in (29) do not depend on $\bar{\mathbf{s}}$ and will not affect the final result in (11). So, from (29), we see that if $\bar{\mathbf{H}}^T \mathbf{Q}^{-1} \bar{\mathbf{H}}$ and $(\bar{\mathbf{H}}^T \mathbf{Q}^{-1} \bar{\mathbf{H}})^{-1} \bar{\mathbf{H}}^T \mathbf{Q}^{-1}$ are precomputed, the matrix-vector multiplications in (12) in the \mathbf{y} -dependent part will be of dimension $n_s \ll N_R$, which is evidently desirable.

We need to evaluate these matrices once for each partitioning (there are N_T of them). This can be done simultaneously in one step. For this purpose, we derive the identities in (30) and (31) where we have defined $\tilde{\Psi}$ and $\tilde{\Psi}^{-1}$ to be diagonal matrices such that $\mathbf{H} \Psi \mathbf{H}^T = \bar{\mathbf{H}} \tilde{\Psi} \bar{\mathbf{H}}^T + \tilde{\mathbf{H}} \tilde{\Psi} \tilde{\mathbf{H}}^T$, and $\bar{\mathbf{P}} \in \{0, 1\}^{N_T \times n_s}$ to be a matrix that has precisely n_s ones such that $\bar{\mathbf{H}} = \mathbf{H} \bar{\mathbf{P}}$ (a column picking matrix). Recall that $\tilde{\Psi}$ is the covariance matrix of $\bar{\mathbf{s}}$. For $n_s = 1$, the identity (30a) (also mentioned in [45], [46]) is well known from the equivalence showed in [47, exerc. 8.18] of the MMSE filter [39, sec. 3.2.1]. Equation (31b) was also derived in [45] and [46] though the derivations there contain a minor error. Specifically, the assumption on $\mathbf{U}\mathbf{U}^T = \mathbf{I}$ in the singular value decomposition of $\mathbf{H} = \mathbf{U}\Sigma\mathbf{V}$ in [46, app. A.2.2] is not valid for $N_R > N_T$.

Now, since we have established (30b) and (31b), we can immediately write

$$\bar{\mathbf{H}}^T \mathbf{Q}^{-1} \bar{\mathbf{H}} = \left(\left(\bar{\mathbf{P}}^T \Psi^{-1} \left(\frac{N_0}{2} \Psi^{-1} + \mathbf{H}^T \mathbf{H} \right)^{-1} \mathbf{H}^T \mathbf{H} \bar{\mathbf{P}} \right)^{-1} - \bar{\Psi} \right)^{-1}, \quad (33)$$

where the innermost inverse is of dimension N_T and the two outermost inversions are of dimension n_s . Focusing on the innermost inverse, it has been observed in [45] that the matrix $\left(\frac{N_0}{2} \Psi^{-1} + \mathbf{H}^T \mathbf{H} \right)$ can be numerically unstable to invert. The reason is that some (diagonal) values in Ψ can be very small. This was addressed in [45] by writing $\Psi^{-1} \left(\frac{N_0}{2} \Psi^{-1} + \mathbf{H}^T \mathbf{H} \right)^{-1} = \left(\frac{N_0}{2} \mathbf{I} + \mathbf{H}^T \mathbf{H} \Psi \right)^{-1}$, which is a more stable inverse but due to the lost symmetry property requires much more operations [48]. We want to facilitate the use of efficient algorithms available for inversion of symmetric matrices [48] but without having to deal with unstable inversions. Therefore, we instead write $\Psi^{-1} \left(\frac{N_0}{2} \Psi^{-1} + \mathbf{H}^T \mathbf{H} \right)^{-1} = \Psi^{-\frac{1}{2}} \left(\frac{N_0}{2} \mathbf{I} + \Psi^{\frac{1}{2}} \mathbf{H}^T \mathbf{H} \Psi^{\frac{1}{2}} \right)^{-1} \Psi^{\frac{1}{2}}$ where $\left(\frac{N_0}{2} \mathbf{I} + \Psi^{\frac{1}{2}} \mathbf{H}^T \mathbf{H} \Psi^{\frac{1}{2}} \right)$ is symmetric and stable to invert. Note that the computation of $\Psi^{\frac{1}{2}}$ and $\Psi^{-\frac{1}{2}}$ is simple, even though it necessitates square root evaluations, since Ψ is diagonal with positive values.

There are several different approaches to inverting a positive definite matrix. Some are more numerically stable than others and some require less operations than others. One very fast and stable approach is through the LDL-decomposition [48, p.139], i.e., $\left(\frac{N_0}{2} \mathbf{I} + \Psi^{\frac{1}{2}} \mathbf{H}^T \mathbf{H} \Psi^{\frac{1}{2}} \right) = \mathbf{L} \mathbf{D} \mathbf{L}^T$, where \mathbf{L} is a lower-triangular matrix with ones on its diagonal and \mathbf{D} is a diagonal matrix with positive diagonal elements. The LDL-decomposition itself requires $N_T^3/3$ operations [48, p.139], and so does the inversion of \mathbf{L} and \mathbf{D} together. Hence, (33) becomes

$$\bar{\mathbf{H}}^T \mathbf{Q}^{-1} \bar{\mathbf{H}} = \left(\left(\bar{\mathbf{P}}^T \Psi^{-\frac{1}{2}} \mathbf{L}^{-T} \mathbf{D}^{-1} \mathbf{L}^{-1} \Psi^{\frac{1}{2}} (\mathbf{H}^T \mathbf{H}) \bar{\mathbf{P}} \right)^{-1} - \bar{\Psi} \right)^{-1}, \quad (34)$$

for which the number of operations for all partitionings can be summarized:

- LDL-decomposition ($N_T^3/3$),
- \mathbf{L}^{-1} ($N_T^3/3$),
- $\Psi^{-\frac{1}{2}} \mathbf{L}^{-T} \mathbf{D}^{-1} \mathbf{L}^{-1} \Psi^{\frac{1}{2}}$ ($N_T^3/3$),
- $\left(\bar{\mathbf{P}}^T \Psi^{-\frac{1}{2}} \mathbf{L}^{-T} \mathbf{D}^{-1} \mathbf{L}^{-1} \Psi^{\frac{1}{2}} (\mathbf{H}^T \mathbf{H}) \bar{\mathbf{P}} \right)^{-1}$ $2n_s^2 N_T^2$.

The remaining evaluations consist of inverses of matrices of very small dimension n_s for which there exist closed form formulas that require a negligible number of operations. Thus, the total number of operations required to compute $\bar{\mathbf{H}}^T \mathbf{Q}^{-1} \bar{\mathbf{H}}$ explicitly for all partitionings is $N_T^3 + 2n_s^2 N_T^2$.

2) *y-dependent processing*: We need to compute, for all partitionings,

$$\begin{aligned} (\bar{\mathbf{H}}^T \mathbf{Q}^{-1} \bar{\mathbf{H}})^{-1} \bar{\mathbf{H}}^T \mathbf{Q}^{-1} \mathbf{y} &\stackrel{(31)}{=} \left(\bar{\mathbf{P}}^T \Psi^{-\frac{1}{2}} \mathbf{L}^{-T} \mathbf{D}^{-1} \mathbf{L}^{-1} \Psi^{\frac{1}{2}} \mathbf{H}^T \mathbf{H} \bar{\mathbf{P}} \right)^{-1} \\ &\quad \times \bar{\mathbf{P}}^T \Psi^{-\frac{1}{2}} \mathbf{L}^{-T} \mathbf{D}^{-1} \mathbf{L}^{-1} \Psi^{\frac{1}{2}} \mathbf{H}^T \mathbf{y}, \end{aligned} \quad (35)$$

where only $\bar{\mathbf{P}}^T \Psi^{-\frac{1}{2}} \mathbf{L}^{-T} \mathbf{D}^{-1} \mathbf{L}^{-1} \Psi^{\frac{1}{2}} \mathbf{H}^T \mathbf{y}$ needs to be evaluated since the leftmost (inverse) matrix in (35) is of dimension n_s and has already been computed in the *y*-independent part. Note that the computation of $\mathbf{H}^T \mathbf{y}$ and subsequently $\Psi^{-\frac{1}{2}} \mathbf{L}^{-T} \mathbf{D}^{-1} \mathbf{L}^{-1} \Psi^{\frac{1}{2}} \mathbf{H}^T \mathbf{y}$ requires $2N_R N_T$ and $2N_T^2$ opera-

tions, respectively. Hence, to compute $(\bar{\mathbf{H}}^T \mathbf{Q}^{-1} \bar{\mathbf{H}})^{-1} \bar{\mathbf{H}}^T \mathbf{Q}^{-1} \mathbf{y}$ for all partitionings requires $2N_R N_T + 2N_T^2$ operations.

To compute (11), for each s_k , requires $n_s^2 2^{n_s}$ operations since the exponents in (12) consist of matrix-vector multiplications of dimension n_s . This, we can safely neglect when $2^{n_s} \ll N_T^2$ (which is typically the case). If higher-order constellations with cardinality much higher than 2 are used, one can keep the cardinality small and fixed by disregarding constellation points outside an appropriately chosen ellipse centered at the mean.

The remaining bottleneck is the computation of the updated covariance matrix $\bar{\mathbf{H}}^T \mathbf{Q}'^{-1} \bar{\mathbf{H}}$ and the update of \mathbf{y} to \mathbf{y}' in (15). The number of operations required for $\bar{\mathbf{H}}^T \mathbf{Q}'^{-1} \bar{\mathbf{H}}$ is $N_T^3 + 2n_s^2 N_T^2$, analogously to the computation of $\bar{\mathbf{H}}^T \mathbf{Q}^{-1} \bar{\mathbf{H}}$. For the update in (15), we have that $\mathbf{y}' = \mathbf{y} - \bar{\mathbf{H}} \mathbb{E}\{\tilde{s}|\mathbf{y}\} = \mathbf{y} - \mathbf{H} \mathbb{E}\{s|\mathbf{y}\} + \bar{\mathbf{H}} \mathbb{E}\{\tilde{s}|\mathbf{y}\}$, which after the transformation in (35) using the updated matrix \mathbf{Q}' instead of \mathbf{Q} becomes

$$\begin{aligned} &(\bar{\mathbf{H}}^T \mathbf{Q}'^{-1} \bar{\mathbf{H}})^{-1} \bar{\mathbf{H}}^T \mathbf{Q}'^{-1} \mathbf{y}' \\ &= (\bar{\mathbf{H}}^T \mathbf{Q}'^{-1} \bar{\mathbf{H}})^{-1} \bar{\mathbf{H}}^T \mathbf{Q}'^{-1} (\mathbf{y} - \mathbf{H} \mathbb{E}\{s|\mathbf{y}\}) + \mathbb{E}\{\tilde{s}|\mathbf{y}\} \\ &= \mathbb{E}\{\tilde{s}|\mathbf{y}\} + \left(\left(\bar{\mathbf{P}}^T \Phi^{-1} \left(\frac{N_0}{2} \Phi^{-1} + \mathbf{H}^T \mathbf{H} \right)^{-1} \mathbf{H}^T \mathbf{H} \bar{\mathbf{P}} \right)^{-1} \right. \\ &\quad \left. \times \bar{\mathbf{P}}^T \Phi^{-1} \left(\frac{N_0}{2} \Phi^{-1} + \mathbf{H}^T \mathbf{H} \right)^{-1} (\mathbf{H}^T \mathbf{y} - \mathbf{H}^T \mathbf{H} \mathbb{E}\{s|\mathbf{y}\}) \right). \end{aligned} \quad (36)$$

The relation between the matrices Φ and $\tilde{\Phi}$ is analogous to the relation between Ψ and $\tilde{\Psi}$. From the discussion after (35), we can conclude that (36) requires $4N_T^2$ operations for all partitionings. Lastly, the LLR computation of each bit requires $n_s^2 2^{n_s}$ operations, which we can safely neglect when $2^{n_s} \ll N_T^2$.

3) *Summary*: Under the assumption that $N_R \geq N_T$ and that no a priori knowledge of s is available, the *y*-independent part of the algorithm requires roughly $N_R N_T^2 + N_T^3 + 2n_s^2 N_T^2$ operations, which is a similar number of operations as required by the soft MMSE algorithm. As for the *y*-dependent part, the number of operations required is roughly $N_T^3 + 2N_R N_T + (2n_s^2 + 6)N_T^2$. Thus, the total number of operations required by the SUMIS detector to evaluate all LLRs associated with one received vector \mathbf{y} is

$$N_R N_T^2 + 2N_T^3 + (4n_s^2 + 6)N_T^2 + 2N_R N_T. \quad (37)$$

The processing in SUMIS that is performed per bit can be done in parallel. The processing (per channel matrix) that involves matrix decompositions and inversions is not as simple to parallelize. More specifically, the LDL (or equivalently the Cholesky) decomposition has an inherent sequential structure that cannot be fully parallelized. Such sequential structures are present in most matrix algebraic operations (e.g., inversions) that are commonly used in detection algorithms. While those operations cannot be fully parallelized, they can be highly parallelized, see [49] and the references therein.

REFERENCES

- [1] E. Telatar, "Capacity of multi-antenna Gaussian channels," *European Transactions on Telecommunications*, vol. 10, no. 6, pp. 585–596, Jun. 2001.

- [2] F. Rusek, D. Persson, B. K. Lau, E. G. Larsson, T. L. Marzetta, O. Edfors, and F. Tufvesson, "Scaling up MIMO: Opportunities and challenges with very large arrays," *IEEE Signal Processing Magazine*, vol. 30, no. 1, pp. 40–60, Jan. 2013.
- [3] N. Srinidhi, T. Datta, A. Chockalingam, and B. S. Rajan, "Layered tabu search algorithm for large-MIMO detection and a lower bound on ML performance," *IEEE Transactions on Communications*, vol. 59, no. 11, pp. 2955–2963, Nov. 2011.
- [4] P. Som, T. Datta, N. Srinidhi, A. Chockalingam, and B. S. Rajan, "Low-complexity detection in large-dimension MIMO-ISI channels using graphical models," *IEEE Journal of Selected Topics in Signal Processing*, vol. 5, no. 8, pp. 1497–1511, Dec. 2011.
- [5] T. Datta, N. Srinidhi, A. Chockalingam, and B. S. Rajan, "Random-restart reactive tabu search algorithm for detection in large-mimo systems," *IEEE Communications Letters*, vol. 14, no. 12, pp. 1107–1109, Dec. 2010.
- [6] P. Li and R. D. Murch, "Multiple output selection-LAS algorithm in large MIMO systems," *IEEE Communications Letters*, vol. 14, no. 5, pp. 399–401, May 2010.
- [7] T. Datta, N. A. Kumar, A. Chockalingam, and B. S. Rajan, "A novel monte carlo sampling based receiver for large-scale uplink multiuser MIMO systems," *IEEE Transactions on Vehicular Technology*, vol. 62, no. 7, pp. 3019–3038, Sept. 2013.
- [8] E. G. Larsson, "MIMO detection methods: How they work," *IEEE Signal Processing Magazine*, vol. 26, no. 3, pp. 91–95, May 2009.
- [9] L. Bai and J. Choi, *Low Complexity MIMO Detection*, Springer, Boston, MA, USA, 2012.
- [10] D. Wübben, D. Seethaler, J. Jaldén, and G. Matz, "Lattice reduction," *IEEE Signal Processing Magazine*, vol. 28, no. 3, pp. 70–91, May 2011.
- [11] A. Elkhazin, K.N. Plataniotis, and S. Pasupathy, "Reduced-dimension map turbo-blast detection," *IEEE Transactions on Communications*, vol. 54, no. 1, pp. 108–118, Jan. 2006.
- [12] E. G. Larsson and J. Jaldén, "Fixed-complexity soft MIMO detection via partial marginalization," *IEEE Transactions on Signal Processing*, vol. 56, no. 8, pp. 3397–3407, Aug. 2008.
- [13] L. G. Barbero and J. S. Thompson, "Extending a fixed-complexity sphere decoder to obtain likelihood information for turbo-MIMO systems," *IEEE Transactions on Vehicular Technology*, vol. 57, no. 5, pp. 2804–2814, Sept. 2008.
- [14] J. W. Choi, B. Shim, A.C. Singer, and N. I. Cho, "Low-complexity decoding via reduced dimension maximum-likelihood search," *IEEE Transactions on Signal Processing*, vol. 58, no. 3, pp. 1780–1793, Mar. 2010.
- [15] E. Viterbo and J. Boutros, "A universal lattice code decoder for fading channels," *IEEE Transactions on Information Theory*, vol. 45, no. 5, pp. 1639–1642, Jul. 1999.
- [16] Z. Guo and P. Nilsson, "Algorithm and implementation of the K-best sphere decoding for MIMO detection," *IEEE Journal on Selected Areas in Communications*, vol. 24, no. 3, pp. 491–503, Mar. 2006.
- [17] G. Papa, D. Ciuonzo, G. Romano, and P. S. Rossi, "Soft-input soft-output king decoder for coded MIMO wireless communications," in *Proc. IEEE 8th International Symposium on Wireless Communication Systems (ISWCS)*, 2011, pp. 760–763.
- [18] C. Studer and H. Bölcskei, "Soft-input soft-output single tree-search sphere decoding," *IEEE Transactions on Information Theory*, vol. 56, no. 10, pp. 4827–4842, Oct. 2010.
- [19] J. W. Choi, B. Shim, and A. C. Singer, "Efficient soft-input soft-output tree detection via an improved path metric," *IEEE Transactions on Information Theory*, vol. 58, pp. 1518–1533, Mar. 2012.
- [20] M. Čirkić, D. Persson, and E. G. Larsson, "Allocation of computational resources for soft MIMO detection," *IEEE Journal of Selected Topics in Signal Processing*, vol. 5, no. 8, pp. 1451–1461, Dec. 2011.
- [21] K. Nikitopoulos and G. Ascheid, "Approximate MIMO iterative processing with adjustable complexity requirements," *IEEE Transactions on Vehicular Technology*, vol. 61, no. 2, pp. 639–650, Feb. 2012.
- [22] D. Taylor, "The estimate feedback equalizer: A suboptimum nonlinear receiver," *IEEE Transactions on Communications*, vol. 21, no. 9, pp. 979–990, Sept. 1973.
- [23] X. Wang and H. V. Poor, "Iterative (turbo) soft interference cancellation and decoding for coded CDMA," *IEEE Transactions on Communications*, vol. 47, no. 7, pp. 1046–1061, Jul. 1999.
- [24] P. Schniter, "Low-complexity equalization of OFDM in doubly selective channels," *IEEE Transactions on Signal Processing*, vol. 52, no. 4, pp. 1002–1011, Apr. 2004.
- [25] W.-J. Choi, K.-W. Cheong, and J. M. Cioffi, "Iterative soft interference cancellation for multiple antenna systems," in *IEEE Wireless Communications and Networking Conference (WCNC)*, Sept. 2000, vol. 1, pp. 304–309.
- [26] J. W. Choi, B. Lee, B. Shim, and I. Kang, "Low complexity detection and precoding for massive MIMO systems," in *Proc. IEEE Wireless Communications and Networking Conference (WCNC)*, Apr. 2013, pp. 2857–2861.
- [27] M. Čirkić and E. G. Larsson, "Near-optimal soft-output fixed-complexity MIMO detection via subspace marginalization and interference suppression," in *Proc. IEEE International Conference on Acoustics, Speech, and Signal Processing*, Mar. 2012, pp. 2805–2808.
- [28] P. Robertson, E. Villebrun, and P. Hoeher, "A comparison of optimal and sub-optimal MAP decoding algorithms operating in the log domain," in *Proc. IEEE International Conference on Communications*, 1995, pp. 1009–1013.
- [29] D. Persson and E. G. Larsson, "Partial marginalization soft MIMO detection with higher order constellations," *IEEE Transactions on Signal Processing*, vol. 59, no. 1, pp. 453–458, Jan. 2011.
- [30] A. D. Murugan, H. El Gamal, M. O. Damen, and G. Caire, "A unified framework for tree search decoding: Rediscovering the sequential decoder," *IEEE Transactions on Information Theory*, vol. 52, no. 3, pp. 933–953, Mar. 2006.
- [31] R. Wang and G. B. Giannakis, "Approaching MIMO channel capacity with soft detection based on hard sphere decoding," *IEEE Transactions on Communications*, vol. 54, no. 4, pp. 587–590, Apr. 2006.
- [32] B. Mennenga, A. von Borany, and G. Fettweis, "Complexity reduced soft-in soft-out sphere detection based on search tuples," in *IEEE International Conference on Communications*, 2009, pp. 1–6.
- [33] B.M. Hochwald and S. ten Brink, "Achieving near-capacity on a multiple-antenna channel," *IEEE Transactions on Communications*, vol. 51, no. 3, pp. 389–399, Mar. 2003.
- [34] J. Jaldén and B. Ottersten, "On the complexity of sphere decoding in digital communications," *IEEE Transactions on Signal Processing*, vol. 53, no. 4, pp. 1474–1484, Apr. 2005.
- [35] L. Rugini, P. Banelli, and S. Caopardi, "A full-rank regularization technique for MMSE detection in multiuser CDMA systems," *IEEE Communications Letters*, vol. 9, no. 1, pp. 34–36, 2005.
- [36] A. Papoulis, *Probability, random variables, and stochastic processes*, McGraw-Hill, USA, 2nd edition, 1984.
- [37] D. Wübben, R. Böhnke, J. Rinas, V. Kühn, and K. D. Kammeyer, "Efficient algorithm for decoding layered space-time codes," *IET Electronics Letters*, vol. 37, no. 22, pp. 1348–1350, Oct. 2001.
- [38] G. Taricco and E. Biglieri, "Space-time decoding with imperfect channel estimation," *IEEE Transactions on Wireless Communications*, vol. 4, no. 4, pp. 1874–1888, Jul. 2005.
- [39] T. Kailath, A. H. Sayed, and B. Hassibi, *Linear Estimation*, Prentice Hall, New Jersey, NJ, USA, 2000.
- [40] S. H. Lee and K. S. Kim, "Design of low-rate irregular LDPC codes using trellis search," *IEEE Transactions on Communications*, vol. 57, no. 7, pp. 1994–2004, Jul. 2009.
- [41] T. J. Richardson and R. L. Urbanke, "The capacity of low-density parity-check codes under message-passing decoding," *IEEE Transactions on Information Theory*, vol. 47, no. 2, pp. 599–618, Feb. 2001.
- [42] T. J. Richardson, M. A. Shokrollahi, and R. L. Urbanke, "Design of capacity-approaching irregular low-density parity-check codes," *IEEE Transactions on Information Theory*, vol. 47, no. 2, pp. 619–637, Feb. 2001.
- [43] D. J.C. Mackay and E. A. Ratzler, "Gallager codes for high rate applications," 2003.
- [44] A. van Zelst and J. S. Hammerschmidt, "A single coefficient spatial correlation model for multiple-input multiple-output (MIMO) radio channels," in *Proc. URSI XXVIII General Assembly*. Citeseer, 2002.
- [45] C. Studer, S. Fateh, and D. Seethaler, "ASIC implementation of soft-input soft-output MIMO detection using MMSE parallel interference cancellation," *IEEE Journal of Solid-State Circuits*, vol. 46, no. 7, pp. 1754–1765, Jul. 2011.
- [46] C. Studer, *Iterative MIMO decoding: Algorithms and VLSI implementation aspects*, Ph.D. thesis, ETH Zürich, Zürich, Switzerland, 2009.
- [47] D. Tse and P. Viswanath, *Fundamentals of wireless communication*, Cambridge Uni. Press, New York, NY, USA, 2005.
- [48] G.H. Golub and C.F. Van Loan, *Matrix computations*, The Johns Hopkins Uni. Press, Baltimore, Maryland, USA, 1996.
- [49] D. Becker, M. Faverge, and J. J. Dongarra, "Towards a parallel tile LDL factorization for multicore architectures," Research rapport, Innovative Computing Laboratory - ICL, 2011.

